The Characterization of Varicella Zoster Virus Specific T Cells In Skin and Blood During Ageing

Milica Vukmanovic-Stejic[1], Daisy Sandhu [1,2], Judith A. Seidel[1], Neil Patel[1,2], Toni O. Sobande [1], Elaine Agius[1,2], Sarah E. Jackson[1], Judilyn Fuentes-Duculan[3], Mayte Suarez-Farinas [3], Neil A. Mabbott[4], Katie E. Lacy[5], Graham Ogg[6] , Frank O Nestle[5], James G. Krueger [3], Malcolm H.A. Rustin [2], Arne N. Akbar [1]

[1]Division of Infection and Immunity, University College London, London, W1T 4JF, England, United Kingdom.

[2] Department of Dermatology, Royal Free Hospital, London, NW3 2QG, England, United Kingdom.

[3]Laboratory for Investigative Dermatology, Rockefeller University, New York, NY 10021, USA

[4]The Roslin Institute and Royal (Dick) School of Veterinary Studies, University of Edinburgh, Easter Bush, Midlothian, EH25 9RG, UK

[5] St. Johns Institute of Dermatology, Guys and St. Thomas' Hospital, London.

[6] MRC Human Immunology Unit, University of Oxford, NIHR Biomedical Research Centre, Oxford, UK

Corresponding author:

Professor Arne N. Akbar, or Dr M Vukmanovic-Stejic, tel: +44-20-31082172/ 02031082173

E-mail: a.akbar@ucl.ac.uk or m.vukmanovic-stejic@ucl.ac.uk

This work was funded by grants from the Medical Research Council, the Biotechnology and Biological Sciences Research Council, The British Skin Foundation and Dermatrust.

Key words: T cell, memory, skin resident, antigen-specific, ageing

Abbreviations: VZV (varicella zoster virus), Treg (regulatory T cells), CMV (cytomegalovirus), HSV (herpes simplex virus),

Running title: Effects of age on VZV specific T cells in blood and skin

ABSTRACT

The varicella-zoster virus (VZV) re-activation increases during ageing. Although the effects of VZV re-activation are observed in the skin (shingles) the number or functional capacity of cutaneous VZV specific T cells have not been investigated. The numbers of circulating IFN-γ secreting VZV specific $CD4^+$ T cells are significantly decreased in old subjects however other measures of VZV-specific $CD4^+$ T cells, including proliferative capacity to VZV antigen stimulation and identification of VZV-specific $CD4^+$ T cells with a MHC class II tetramer (epitope of IE-63 protein), were similar in both age groups. The majority of T cells in the skin of both age groups expressed CD69, a characteristic of skin resident T cells. VZV-specific $CD4^+$ T cells were significantly increased in the skin compared to the blood in young and old subjects and their function was similar in both age groups. In contrast the number of $Foxp3^+$ regulatory T cells (Tregs) and expression of the inhibitory receptor PD-1 on $CD4^+$ T cells were significantly increased in the skin of older humans. Therefore VZV-specific $CD4^+$ T cells in the skin of older individuals are functionally competent. However their activity may be restricted by multiple inhibitory influences *in situ*.

INTRODUCTION

Varicella zoster virus (VZV), an alpha-herpes virus, is the causative agent of chickenpox. After resolution of the initial infection VZV enters a latent phase within dorsal root ganglia. However, later in life VZV re-activation can occur, causing herpes zoster (also known as shingles) that results from virus shedding into the skin (Arvin, 1996; Arvin, 2001; Goldblatt, 1998). Although the skin is the major site that is involved in VZV reactivation during shingles, it is not clear if this is related to changes in skin resident VZV specific T cells in this tissue. The role of a subset of memory cells in the skin, termed tissue resident memory T cells (Trm), that are poised to provide efficient and rapid immunity in this organ has been described recently (Gebhardt *et al.*, 2009; Gebhardt *et al.*, 2011; Jiang *et al.*, 2012). These Trm cells have been shown to be part of the first line of defence against herpes simplex virus (HSV) or human papiloma virus (HPV) infections (Cuburu *et al.*, 2012; Gebhardt *et al.*, 2009; Mackay *et al.*, 2012; Masopust *et al.*, 2010; Tang and Rosenthal, 2010). The activation of these cells also enables the recruitment of circulating antigen-specific T cells that amplifies the response (Schenkel *et al.*, 2013). Although most studies of Trm have focused on $CD8^+$ populations (especially in mice), $CD4^+$ Trm cells also reside in the skin (Clark *et al.*, 2006; Clark *et al.*, 2012; Mueller *et al.*, 2013). In addition to the tissue resident Trm cells, skin also contains recirculating memory T cells which actively recirculate between blood, skin and lymphoid organs (Bromley *et al.*, 2013; Clark *et al.*, 2012; Jiang *et al.*, 2012). It has been proposed that non-migrating tissue resident T cells express CD69 which was found to be necessary for S1P1 down-regulation and T cell retention (Carbone *et al.*, 2013; Skon *et al.*, 2013).

We have investigated quantitative and qualitative changes in VZV specific $CD4^+$ T cells in the blood and skin in young and old subjects and showed that although the numbers of these cells were increased in the skin compared to the blood, the capacity of these cells to secrete

cytokines was not altered by ageing. The vast majority of T cells in the skin of both young and old individuals expressed CD69, a marker for tissue resident memory T cell populations (Clark *et al.*, 2012; Gebhardt *et al.*, 2009; Jiang *et al.*, 2012) suggesting that VZV-specific $CD4^+$ T cells in healthy skin may be Trm cells. Although cutaneous VZV specific T cells in old individuals are functionally competent, previous studies have shown that these subjects have decreased ability to mount a recall antigen responses to cutaneous VZV antigen challenge (Agius *et al.*, 2009; Levin *et al.*, 2003). Our results suggest that this decrease in cutaneous VZV-specific immunity in the tissue is not directly due to a defect in $CD4^+$ Trm cells. Instead, external influences such as the increased numbers of suppressive Tregs (Agius *et al.*, 2009; Seneschal *et al.*, 2012) and/or increased signalling through the inhibitory receptor PD-1 (Wherry, 2011; Zajac *et al.*, 1998), that is highly expressed on skin resident $CD4^+$ T cells, may create an inhibitory microenvironment that restricts effective immune responses to VZV in the skin of older humans.

RESULTS

VZV specific $CD4^+$T cells in the blood during ageing

We investigated the effect of increasing age on VZV specific $CD4^+$ T cell frequency by measuring IFN-γ and IL-2 responses following overnight stimulation of PBMC with VZV lysate. 133 donors were analysed (aged 20-91 years) and only donors serologically positive for VZV were included in the analysis. Figure 1A (left panel) shows representative dot plots of IFN-γ production for unstimulated and VZV stimulated PBMC gated on $CD3^+CD4^+$ T cells. We found a significant decrease of IFN-γ secreting cells during ageing (Figure 1A right panel, $p<0.0001$) confirming previous reports (Asanuma *et al.*, 2000; Levin *et al.*, 2003). We also examined the IL-2 responses to VZV of the donors analysed (Supplementary Figure 1) but found that host age did not significantly influence the frequency of IL-2 secreting cells.

We next investigated VZV specific T cell activity by assessing the ability of PBMC from young and old donors to proliferate after VZV antigen stimulation *in vitro* (Figure 1B, 1C). After 6 days of stimulation with a range of concentrations of VZV lysate (n=29 old and 26 young) the extent of proliferation measured by ^{3}H-thymidine uptake was similar in young and old subjects except at the lowest dose of VZV antigen used (Figure 1B). Furthermore there were no differences in proportions of cells expressing Ki67 three days after VZV lysate stimulation (4 µl/ml) *in vitro* (Figure 1C). This indicates that the decrease in VZV specific cells, identified by IFN-γ secretion in the peripheral blood compartment, does not represent a global defect in the functional responses of these cells.

We also investigated the frequency of VZV specific cells in young and old subjects (Figure 1D) using a class II tetramer HLA-DRB1*1501 restricted IE63 tetramer (Jones *et al.*, 2007; Vukmanovic-Stejic *et al.*, 2013). No difference was observed in the number of tetramer

positive VZV specific $CD4^+$ T cells between the young and old individuals tested (Figure 1D). We confirmed that the tetramer staining was specific by showing an absence of staining when a control tetramer (CLIP) was used, and also when HLA DRB1*1501-negative individuals were tested (data not shown and (Vukmanovic-Stejic *et al.*, 2013)).

Effect of age on leukocyte populations and global gene expression signatures in the skin

We investigated if there were numerical or functional differences in the T cells found in young and old skin. We collected 5 mm punch biopsies from individuals of both age groups and analysed them by immunohistochemistry and immunofluorescence using antibodies specific for CD3, CD4, CD11c, CD163 and Foxp3 (Figure 2A). No difference was observed in the number of $CD3^+$, $CD4^+$ or $CD8^+$ T cells with age (Figure 2B, Table 1). The numbers of dermal dendritic cells (CD11c) or macrophages (CD163) (Haniffa *et al.*, 2009; Zaba *et al.*, 2007; Zaba *et al.*, 2008) were also unaffected by increasing age (Figure 2B, Table 1). However there were significantly increased numbers of $CD4^+Foxp3^+$ T cells in the skin of old compared to young individuals in agreement with previous studies (Agius *et al.*, 2009; Gregg *et al.*, 2005; Lages *et al.*, 2008). This difference was also observed by flow cytometric analysis of skin derived populations (Supplementary Figure 2A) The increased proportion of $Foxp3^+$ cells in the old skin is significantly correlated with a decrease of memory $CD4^+$ T cell infiltration and with the decrease in the clinical response after intradermal challenge with VZV antigen (Figure 2C, Supplementary Figure 2) confirming previous observations (Agius *et al.*, 2009; Vukmanovic-Stejic *et al.*, 2013). This is indirect evidence that these cells in older subjects have suppressive activity.

We next investigated global gene expression profiles in the skin of young and old subjects. Transcriptional analysis was performed on the skin biopsies of normal skin collected from 7

young and 7 healthy old individuals. Overall, unsupervised clustering coupled with bootstrapping did not identify stable clusters separating skin samples from young and old individuals (Figure 2D and Supplementary Figure 3A). Only 2 genes were considered differentially expressed *LPPR4* (higher in young) and *ADAMTSL1* (higher in old) using a typical FDR<0.05 and FCH>2. In terms of pathways, Gene Set Variation Analysis (GSVA) suggested differences in human skin pigmentation genes and cell cycle related genes (Wang *et al.*, 2013) but not in terms of immune genes, positive or negative regulators or in any of the skin specific cytokine pathways that we have curated (Suarez-Farinas *et al.*, 2011) (Supplementary Figure 2C).

Next, the global gene expression profiles in the young and aged skin samples were compared with that of a large collection of microarray data sets from distinct human primary cell populations (745 individual data sets) (Mabbott *et al.*, 2013). Data were analysed using Biolayout Express^{3D} with a Pearson correlation r=0.90 and Markov cluster (MCL) of 2.2,, and generated 140 clusters of ≥6 probe sets (genes). The network graph's structure is derived from the clustering of genes that are expressed in a cell- or function-specific manner (Supplementary Figure 3D; Supplementary Table 1) and their contents reflect the nature of the cell populations represented in human skin. Congruent with the differential transcriptional analyses presented above (Supplementary Figure 3B, C), no significant difference was observed in the expression levels of the genes within these cell-specific (eg: keratinocytes, endothelium) and cellular activity-related clusters (eg: extracellular matrix, MHC genes) between the two age groups (Supplementary Figure 3E).

Effect of age on the extent of differentiation of CD4 T cells in blood and skin.

We investigated whether the T cells in skin were true skin resident T cells as defined by CD69 expression that is a marker for tissue retention(Clark *et al.*, 2012; Gebhardt *et al.*, 2009; Jiang *et al.*, 2012; Skon *et al.*, 2013), In contrast to circulating T cells 80-90% of skin derived CD4 (Figure 3A, 3B) and CD8 populations (data not shown) express CD69. In addition, only around 10% of skin derived cells express CCR7 confirming that the vast majority of cutaneous T cells are skin resident and not transient T cell populations (Clark *et al.*, 2012; Gebhardt *et al.*, 2009; Jiang *et al.*, 2012). Furthermore $CD69^+$ T cells did not express surface CD25 suggesting they were not an activated population and this was also confirmed by their small size, defined by forward and side scatter properties by flow cytometry. There was no significant change in the proportion of $CD69^+$ cells with age (Figure 3B).

To determine whether excessive differentiation towards an end stage could reflect altered T cell function in the skin compared to T cells in peripheral blood we collected paired blood and skin samples from young and old individuals (n=23 old and n=31 young for CD4, n=10 old and 14 young for CD8). Based on their expression of surface CD45RA, CD27, CD4 (Figure 3C, D) and CD8 (Supplementary Figure 4A, B) T cells from both blood and skin can be subdivided into 4 subsets. The $CD45RA^+CD27^+$ population is the least differentiated and has the longest telomeres, $CD45RA^-CD27^+$ cells have intermediated telomere lengths while both $CD45RA^-CD27^-$ and $CD45RA^+CD27^-$ cells have relatively short telomeres and express multiple other characteristics of senescence (Di Mitri *et al.*, 2011; Henson *et al.*, 2014; Libri *et al.*, 2011). In both young and old subjects, cutaneous T cells in both $CD4^+$ (Figure 3C, D) and $CD8^+$ populations (Supplementary Figure 4A, B) showed a significant decrease in the undifferentiated $CD45RA^+CD27^+$ population with a concomitant increase in $CD27^+CD45RA^-$ and $CD45RA^-CD27^-$ cells. In older subjects, the proportion of $CD45RA^-CD27^-$ cells was

significantly higher within skin CD4 and CD8 compartments compared to young subjects (Figure 3).

We next investigated the functional capacity of skin resident T cells isolated from punch biopsies. Following a 6 hour stimulation with PMA and ionomycin cells were stained for IL-2, IFN-γ, TNF-α and IL-22. There were no significant differences in the capacity of $CD4^+$ (Figure 3 E, F) or $CD8^+$ T cells from the skin of young and old individuals to secrete these inflammatory cytokines after stimulation *in vitro* (Supplementary Figure4, D).

VZV-specific skin resident T cells in young and old subjects.

We next investigated the phenotypic and functional characteristics of VZV specific T cells in both the skin and blood of young and old subjects. Skin T cells isolated from punch biopsies, and paired blood samples, were tested for their ability to synthesize IFN-γ, TNF-α and/or IL-2 after overnight re-stimulation with VZV lysate as previously described (Vukmanovic-Stejic *et al.*, 2013). Minimal IFN-γ or IL-2 was produced by blood or skin $CD4^+$ T cells in the control cultures without added VZV antigens (not shown). We could identify cytokine producing $CD4^+$ cells in skin of > 60% of young and old individuals tested (positive staining for one or more cytokines, Figure 4A). In those individuals where VZV specific cells were found in both compartments, there were significantly higher proportions of these cells in the skin (Figure 4A, 4B, p=0.001, Wilcoxon paired test, n=9 old and 15 young). The observed difference was not accounted for by the difference in the differentiation state of skin versus blood CD4 T cells as there was a significantly increased proportion of VZV-specific cells in skin compared to the circulating memory compartment. When the proportion of cytokine secreting VZV-specific $CD4^+$ cells was compared between the skin of young and old individuals, no significant difference was observed (Figure 4C). Therefore there is no obvious

age-associated reduction in the number of cytokine secreting VZV specific $CD4^+$ T cells in the skin.

We also investigated the characteristics of VZV specific $CD4^+$ T cells in the skin that were identified by class II tetramer binding. Paired samples of cells isolated from skin biopsies and PBMC were stained with an HLA-DRB1*1501 restricted IE63 tetramer (Jones *et al.*, 2007). The representative tetramer staining is shown in Figure 4D (left panels). Increased proportions of VZV-specific $CD4^+$ T cells were detected in the skin when compared to the blood in both old and young individuals (Figure 4D, Wilcoxon paired test, p=0.06 in young n=6; and p=0.008 in the old; n=5). The specificity of tetramer staining was confirmed as described above (Vukmanovic-Stejic *et al.*, 2013). Therefore, using either intracellular cytokine staining or tetramer binding we found higher proportions of VZV specific $CD4^+$ T cells in the skin than in blood of both young and old individuals, however there were no differences between the age groups in either compartment.

We next compared the differentiation state of skin resident VZV specific $CD4^+$ T cells between young and old individuals. Overall, VZV specific cells identified in the skin are predominantly of the $CD45RA^-CD27^+$ and $CD45RA^-CD27^-$ phenotype (Figure 4E) similar to that seen in blood (Supplementary Fig 5) in both age groups. Furthermore there was a significant increase in $CD45RA^+CD27^-$ T cells, that have characteristics of end-stage differentiation or senescence (Di Mitri *et al.*, 2011; Henson *et al.*, 2014; Libri *et al.*, 2011) within the VZV-specific population in the old compared to young skin. The phenotype of tetramer positive cells in skin was similar to that observed when cytokine secreting VZV specific cells were analysed (Supplementary Fig 5C). In conclusion, VZV specific $CD4^+$ T cells in blood and in skin are functional and are not restricted by excessive differentiation.

Expression of PD-1 in skin during ageing:

Since the numbers of skin resident VZV specific $CD4^+$ T cells are not decreased during ageing and they are able to secrete cytokines in response to VZV antigen challenge *in vitro*, other factors may contribute to the impaired skin recall response to VZV antigen challenge in older subjects and to their increased susceptibility to shingles (Agius *et al.*, 2009; Levin *et al.*, 2003; Tang *et al.*, 2012; Weinberg *et al.*, 2010). The progressive loss of cytokine production and proliferative activity by $CD4^+$ T cells as a result of chronic immune stimulation during persistent viral infections and cancer is associated with the expression of PD-1 and other inhibitory receptors (Wherry, 2011; Zajac *et al.*, 1998). Blockade of these receptors can reverse these functional defects in these cells (Kamphorst and Ahmed, 2013). We therefore investigated whether there was increased expression of the T cell surface inhibitory receptor PD-1 in blood compared to skin cells during ageing. Paired blood and normal skin samples stained for the expression of PD-1 on CD4 (n= 17; 6 young, 6 middle aged, 5 old) and CD8+ T cells (n=-12; 4 young, 3 middle aged, 5 old). (Figure 5A, B). There was a highly significant increase in PD-1 expression on skin resident compared to circulating T cells ($p < 0.001$, Wilcoxon paired test). PD-1 expression was increased in both blood and skin during ageing (Figure 5C) with as many as 40% of CD4+ T cells being positive in the skin. This data suggests that T cells in the skin of old humans may be more susceptible to inhibition through PD-1 signalling.

DISCUSSION

Recent studies have shown that skin resident memory T (Trm) cells play an important role in providing protection against re-exposure to, or re-activation of, local persisting pathogens (Clark *et al.*, 2012; Cuburu *et al.*, 2012; Gebhardt *et al.*, 2009; Mackay *et al.*, 2012; Masopust *et al.*, 2010; Mueller *et al.*, 2013; Tang and Rosenthal, 2010). Furthermore, these Trm cell populations may be regulated independently of the circulating memory T cell pools of cells (Carbone *et al.*, 2013; Clark *et al.*, 2012; Gebhardt *et al.*, 2011; Mueller *et al.*, 2013; Schenkel *et al.*, 2013). Considering the skin manifestation of both primary and secondary varicella disease, it is unusual that VZV specific T cells have only previously been studied in the peripheral blood (Asanuma *et al.*, 2000; Hayward and Herberger, 1987; Patterson-Bartlett *et al.*, 2007; van Besouw *et al.*, 2012; Weinberg and Levin, 2010). We first investigated whether there was a general decrease in the number or functional capacity of skin resident T cells in older subjects. Based on the expression of CD69, that was expressed by almost all skin derived CD4 and CD8 T cells, together with the lack of CCR7 expression and the fact that skin biopsies were collected from normal, unchallenged skin we concluded that our skin derived cells represent a skin resident population (Clark *et al.*, 2012; Gebhardt *et al.*, 2009; Jiang *et al.*, 2012; Skon *et al.*, 2013). However contribution of recirculating T cells transiently patrolling the skin cannot be completely discounted (Zhu *et al.*, 2013). A key observation was that there were significantly more VZV specific $CD4^+$ T cells in the skin compared to the blood in both young and old individuals. Since the skin contains more T cells than the blood (Clark, 2010; Clark *et al.*, 2006), the decrease in VZV-specific T cells in the circulation during ageing may not represent a global decrease of these cells *in vivo* as they may simply have re-located to the skin. This observation coupled to the fact that other methods of evaluating VZV-specific T cells do not indicate a reduction of these cells in the

blood suggests that there may not be a general defect of VZV-specific T cell numbers or function during ageing.

We found no differences in numbers of dendritic cells and macrophages between both age groups, and transcriptional profiling of young and old normal skin did not show any significant differences in the genes involved in mononuclear phagocyte function or immune responses. Therefore the general skin microenvironment at a steady state appears very similar in young and old individuals suggesting that the reduced recall response to antigen in the skin during ageing (Agius *et al.*, 2009) probably occurs downstream of antigen challenge.

We investigated whether Trm cells in the skin of older humans were inhibited *in situ*, as this could explain why there is a reduced recall response to VZV skin test antigen challenge and also the predisposition to VZV reactivation *in vivo*. We showed previously that $Foxp3^+$ Tregs that are identified in the skin are suppressive and there is a significant inverse correlation between the number of these cells present and the size of the delayed type hypersensitivity response after VZV challenge ((Vukmanovic-Stejic *et al.*, 2013) and Figure 2C, Supplementary Figure 2). The increase in Tregs during ageing has also been observed in the blood of normal subjects (Gregg *et al.*, 2005; Vukmanovic-Stejic *et al.*, 2006) and has also been reported in the tissues of old mice (Lages *et al.*, 2008; Raynor *et al.*, 2012). This supports the possibility that the increase in Treg cell numbers and their suppressive activity may contribute to decreased VZV specific responses in older subjects.

Signalling through PD-1 and other inhibitory receptors can inhibit T cell responses both *in vitro* and *in vivo* (Wherry, 2011; Zajac *et al.*, 1998). The blockade of these receptors can reverse these functional defects in these cells and this has led to the use of PD-1 blocking

strategies in the treatment of melanoma and other skin cancers (Flemming, 2012; Kamphorst and Ahmed, 2013; Lu *et al.*, 2014). In addition, it has been shown recently that interplay between Tregs and PD-1 signalling regulates immune responsiveness and the control of viral infection *in vivo* (Penaloza-MacMaster *et al.*, 2014). We observed very high PD-1 expression on skin compared to blood T cells that increased with age. This suggests that inhibitory signalling by different mechanisms may actively regulate immune responsiveness in the skin, especially during ageing. The reason for the increase in Treg numbers or PD-1 expression in the skin during ageing is unclear. It has been shown previously that infection with persistent viruses such as CMV in humans can induce PD-1 expression and it is possible that more of the old subjects we have studied are CMV^+ than the young cohort (Henson *et al.*, 2014). Alternatively, these changes may be linked to the increased inflammation (inflammageing) that is observed in elderly subjects (Franceschi *et al.*, 2000).

Our studies highlight the importance of studying human immunity in additional compartments to peripheral blood. The availability of a vaccine (Zostavax) to prevent herpes zoster in older subjects has reduced the incidence of shingles in the elderly (Gershon, 2007; Levin *et al.*, 2008; Weinberg *et al.*, 2009) although efficacy of the vaccine is only 38% in the very old (>80yrs). This indicates that it is essential to study the mechanisms that are responsible for the declining immunity during ageing to rationalize ways by which immunity in general and vaccine responses in particular could be improved in the elderly.

MATERIALS AND METHODS

Subjects: Healthy individuals who had a history of previous chickenpox infection (n=94, median age = 32.5 years, age range 20-92 years, 38 male, 56 female) were recruited for the study. Subjects were grouped as young <40, middle aged 40-65 and old >60 years old. This work was approved by the Ethics Committee of the Royal Free Hospital, London. All volunteers provided written informed consent and study procedures were performed in accordance with the principles of the declaration of Helsinki. Individuals with history of neoplasia, immunosuppressive disorders or inflammatory skin disorders and individuals on immunosuppressive medication were excluded. In some cases skin from healthy individuals was obtained from donors undergoing routine plastic surgery at Guy's and St. Thomas' hospitals (approved by the Institutional Review Board of Guy's Hospital). To examine the clinical response to VZV, healthy individuals were injected intradermally with Varicella Zoster Virus (VZV) skin test antigen from The Research Foundation for Microbial Diseases of Osaka University (BIKEN) as described previously(Agius *et al.*, 2009; Vukmanovic-Stejic *et al.*, 2011).

Skin biopsies: Punch biopsies (5 mm diameter) from the upper volar region of the forearm were obtained from 30 young and 25 old volunteers. Biopsies were frozen in optimal cutting temperature compound (OCT, Bright Instrument Company Ltd, Huntingdon, Uk). 6 μm sections were cut and then fixed in ethanol and acetone and stored at -80ºC. For functional analysis of skin cells 5 mm punch biopsies were digested overnight with 0.8mg/ml of collagenase IV (Sigma Aldrich, Gillingham, UK) as described (Vukmanovic-Stejic *et al.*, 2013). For the analysis of the DTH response to VZV challenge skin biopsies were collected at different times post injection, frozen and used for histological analysis (Agius *et al.*, 2009).

PBMC preparation: Heparinized blood samples were collected from healthy volunteers and patients with acute disease. PBMCs were prepared by density centrifugation on Ficoll-Paque (Amersham Biosciences, Little Chalfont, UK) and re-suspended in complete medium.

Flow Cytometric Analysis: Multi-parameter analysis of skin and blood T cell phenotype was performed on LSR II or BD Fortessa using FACS Diva software (both BD Biosciences, Oxford, UK) and further analyzed using FlowJo software (TreeStar, Inc) as previously described (Agius *et al.*, 2009; Vukmanovic-Stejic *et al.*, 2013). PBMCs or skin cells were stained with different combinations of antibodies including CD3, CD4, CD8, CD45RA, CD28, CD27 (BD Biosciences) Ki67, CLA, CCR7 and PD-1 (clone EH12.2H7; Biolegend, London, UK). All surface staining was performed for 30 minutes on ice. Isotype control staining and FMO controls were used to set the quadrants. Ki67 staining (clone B56, BD Bioscience) was performed by intracellular staining using the Foxp3 Staining Buffer Set (Miltenyi Biotec, Bisley, UK). For intracellular cytokine staining cells were stimulated with VZV lysate (Virusys corporation, Taneytown, MD) or SEB as positive control and incubated for 15 hours at 37°C, 5% CO2 in the presence of 5 µg/ml Brefeldin A (Sigma-Aldrich, Gillingham, UK). Unstimulated controls were always included. Following stimulations cells were stained for surface markers for 30 minutes at 4^{o}C, washed, fixed and permeabilised (Fix & Perm Cell Permeabilisation Kit, Invitrogen, Paisley, UK) before staining for IL-2, IFN-γ and TNF-α (all from BD Biosciences, Oxford, UK).

Tetramer staining Tetramer staining was performed as previously described using DRB1*1501 iTAg MHCII tetramer complexed to VZV IE63 peptide 24 (QRAIERYAGAETAEY) (Beckman Coulter, High Wycombe, UK); CLIP peptide (PVSKMRMATPLLMQA) was used as a control (Jones *et al.*, 2007; Vukmanovic-Stejic *et al.*, 2013). Briefly, cells were first incubated with 2 µg/ml HLA Class II tetramers for 1-2

hours at 37^{o}C in the dark, washed in PBS and then stained for different surface markers as needed. We analysed the tetramer expression within the CD4^{+} T cell subset by gating on the lymphocytes and excluding B cells, monocytes and dead cells (Via-Probe positive population).

Immunofluorescence: 6 µm skin sections collected from normal or VZV injected skin were blocked with Dako non-serum protein block for 20 minutes, followed by incubation with primary antibodies (biotin anti-human Foxp3 and mouse anti- human CD4) overnight at 4^{o}C, followed by incubation with strepCy3 and anti-mouse IgG1 Alexa Fluor 488 for 1hr at room temperature as described (Vukmanovic-Stejic *et al.*, 2008). Cell numbers were expressed as the mean absolute cell number per perivascular infiltrate where 5 largest perivascular infiltrates present in the upper and mid dermis of each section were counted (Vukmanovic-Stejic *et al.*, 2008).

Immunohistochemistry: Skin sections from normal skin (n=6 young, n=6 old) were stained with purified mouse anti-human CD3 antibody, purified mouse anti-human CD8 antibody (both Dakocytomation, Ely, UK), purified mouse anti-human CD4 and CD11c antibodies (BD Biosciences, Oxford, UK) or purified mouse anti-human CD163 antibody (Acris, Herford, Germany). Sections were counterstained using rabbit anti-mouse horseradish-peroxidase conjugated antibody (Dakocytomation, Ely, UK) and immunostaining revealed using chromagen 3'-diaminobenzidine tetrahydrochloride. The number of positive cells/mm^{2} was counted manually using computer-assisted image analysis (NIH Image 6.1; http://rsb.info.nih.gov/nih-image).

Transcriptional analysis: 3 mm punch biopsies were collected from young and old individuals and immediately frozen in RNAlater and stored at –20^{o}C until use. Tissues were homogenized and total RNA extracted using RNeasy Mini Kit (Qiagen, Manchester, UK). Target

amplification and labelling was performed according to standard protocols using Nugen Ovation WB Kit. RNA was hybridized to Affymetrix Human Genome U133 2.0 plus arrays. Affymetrix gene chips were scanned for spatial artefacts using the Hirshlight package (Suarez-Farinas *et al.*, 2005). Gene expression measures were obtained using the GCRMA algorithm (Wu and Irizarry, 2004). Group comparisons were made using the moderated t-test and P-values were adjusted for multiple hypotheses using the Benjamini-Hochberg procedure.

Network analysis of the genes expressed within skin samples and in various human cell populations was performed as described previously (Mabbott *et al.*, 2013). Briefly, human skin-punch microarray data were combined with a large collection of other primary cell gene-expression data sets (745 individual microarray data sets), available from the GEO database on the Affymetrix Human Genome U133 Plus 2.0 expression array platform (GSE49910) and analysed using Biolayout Express^{3D} software (Freeman *et al.*, 2007). The graph of these data was then explored to understand the significance of the gene clusters, identify those expressed by the young and old skin samples and their functional relationships to the other cell populations represented.

Statistics: Statistical analysis was performed using GraphPad Prism version 6.00 for Windows (GraphPad Software, San Diego, California, USA). Non-parametric tests were predominantly utilised as data sets were not normally distributed. The Wilcoxon matched pairs test or a paired t-test was used when comparing two groups of matched data and a 2-tailed Mann-Whitney test was used when comparing two unpaired groups.

Conflict-of-interest disclosure: The authors declare no competing financial interests.

References

Agius E, Lacy KE, Vukmanovic-Stejic M*, et al.* (2009) Decreased TNF-{alpha} synthesis by macrophages restricts cutaneous immunosurveillance by memory CD4+ T cells during aging. *The Journal of Experimental Medicine* 206:1929-40.

Arvin AM (1996) Varicella-zoster virus. *ClinMicrobiolRev* 9:361-81.

Arvin AM (2001) Varicella-zoster virus: molecular virology and virus-host interactions. *Current opinion in microbiology* 4:442-9.

Asanuma H, Sharp M, Maecker HT*, et al.* (2000) Frequencies of memory T cells specific for varicella-zoster virus, herpes simplex virus, and cytomegalovirus by intracellular detection of cytokine expression. *JInfectDis* 181:859-66.

Bromley SK, Yan S, Tomura M*, et al.* (2013) Recirculating memory T cells are a unique subset of CD4+ T cells with a distinct phenotype and migratory pattern. *J Immunol* 190:970-6.

Carbone FR, Mackay LK, Heath WR*, et al.* (2013) Distinct resident and recirculating memory T cell subsets in non-lymphoid tissues. *Curr Opin Immunol* 25:329-33.

Clark RA (2010) Skin-resident T cells: the ups and downs of on site immunity. *J Invest Dermatol* 130:362-70.

Clark RA, Chong B, Mirchandani N*, et al.* (2006) The vast majority of CLA+ T cells are resident in normal skin. *J Immunol* 176:4431-9.

Clark RA, Watanabe R, Teague JE*, et al.* (2012) Skin effector memory T cells do not recirculate and provide immune protection in alemtuzumab-treated CTCL patients. *SciTranslMed* 4:117ra7.

Cuburu N, Graham BS, Buck CB*, et al.* (2012) Intravaginal immunization with HPV vectors induces tissue-resident CD8+ T cell responses. *The Journal of clinical investigation* 122:4606-20.

Di Mitri D, Azevedo RI, Henson SM*, et al.* (2011) Reversible senescence in human CD4+CD45RA+. *JImmunol* 187:2093-100.

Flemming A (2012) Cancer: PD1 makes waves in anticancer immunotherapy. *Nature reviews Drug discovery* 11:601.

Franceschi C, Bonafe M, Valensin S*, et al.* (2000) Inflamm-aging. An evolutionary perspective on immunosenescence. *Annals of the New York Academy of Sciences* 908:244-54.

Freeman TC, Goldovsky L, Brosch M*, et al.* (2007) Construction, visualisation, and clustering of transcription networks from microarray expression data. *PLoS computational biology* 3:2032-42.

Gebhardt T, Wakim LM, Eidsmo L*, et al.* (2009) Memory T cells in nonlymphoid tissue that provide enhanced local immunity during infection with herpes simplex virus. *NatImmunol* 10:524-30.

Gebhardt T, Whitney PG, Zaid A*, et al.* (2011) Different patterns of peripheral migration by memory CD4+ and CD8+ T cells. *Nature* 477:216-9.

Gershon AA (2007) Varicella-zoster vaccine.

Goldblatt D (1998) The immunology of chickenpox. A review prepared for the UK Advisory Group on Chickenpox on behalf of the British Society for the Study of Infection. *The Journal of infection* 36 Suppl 1:11-6.

Gregg R, Smith CM, Clark FJ*, et al.* (2005) The number of human peripheral blood CD4+ CD25high regulatory T cells increases with age. *ClinExpImmunol* 140:540-6.

Haniffa M, Ginhoux F, Wang X-N*, et al.* (2009) Differential rates of replacement of human dermal dendritic cells and macrophages during hematopoietic stem cell transplantation. *The Journal of Experimental Medicine* 206:371-85.

Hayward AR, Herberger M (1987) Lymphocyte responses to varicella zoster virus in the elderly. *Journal of clinical immunology* 7:174-8.

Henson SM, Lanna A, Riddell NE*, et al.* (2014) p38 signaling inhibits mTORC1-independent autophagy in senescent human CD8+ T cells. *The Journal of clinical investigation* 124:4004-16.

Jiang X, Clark RA, Liu L*, et al.* (2012) Skin infection generates non-migratory memory CD8+ TRM cells providing global skin immunity. *Nature* 483:227-31.

Jones L, Black AP, Malavige GN*, et al.* (2007) Phenotypic analysis of human CD4+ T cells specific for immediate-early 63 protein of varicella-zoster virus. *EurJ Immunol* 37:3393-403.

Kamphorst AO, Ahmed R (2013) Manipulating the PD-1 pathway to improve immunity. *Curr Opin Immunol* 25:381-8.

Lages CS, Suffia I, Velilla PA*, et al.* (2008) Functional regulatory T cells accumulate in aged hosts and promote chronic infectious disease reactivation. *J Immunol* 181:1835-48.

Levin MJ, Oxman MN, Zhang JH*, et al.* (2008) Varicella-zoster virus-specific immune responses in elderly recipients of a herpes zoster vaccine. *The Journal of infectious diseases* 197:825-35.

Levin MJ, Smith JG, Kaufhold RM*, et al.* (2003) Decline in varicella-zoster virus (VZV)-specific cell-mediated immunity with increasing age and boosting with a high-dose VZV vaccine. *JInfectDis* 188:1336-44.

Libri V, Azevedo RI, Jackson SE*, et al.* (2011) Cytomegalovirus infection induces the accumulation of short-lived, multifunctional CD4+CD45RA+CD27+ T cells: the potential involvement of interleukin-7 in this process. *Immunology* 132:326-39.

Lu J, Lee-Gabel L, Nadeau MC*, et al.* (2014) Clinical evaluation of compounds targeting PD-1/PD-L1 pathway for cancer immunotherapy. *Journal of oncology pharmacy practice : official publication of the International Society of Oncology Pharmacy Practitioners*.

Mabbott NA, Baillie JK, Brown H*, et al.* (2013) An expression atlas of human primary cells: inference of gene function from coexpression networks. *BMC genomics* 14:632.

Mackay LK, Stock AT, Ma JZ*, et al.* (2012) Long-lived epithelial immunity by tissue-resident memory T (TRM) cells in the absence of persisting local antigen presentation. *Proceedings of the National Academy of Sciences* 109:7037-42.

Masopust D, Choo D, Vezys V*, et al.* (2010) Dynamic T cell migration program provides resident memory within intestinal epithelium. *J Exp Med* 207:553-64.

Mueller SN, Gebhardt T, Carbone FR*, et al.* (2013) Memory T cell subsets, migration patterns, and tissue residence. *Annu Rev Immunol* 31:137-61.

Patterson-Bartlett J, Levin MJ, Lang N*, et al.* (2007) Phenotypic and functional characterization of ex vivo T cell responses to the live attenuated herpes zoster vaccine. *Vaccine* 25:7087-93.

Penaloza-MacMaster P, Kamphorst AO, Wieland A*, et al.* (2014) Interplay between regulatory T cells and PD-1 in modulating T cell exhaustion and viral control during chronic LCMV infection. *J Exp Med* 211:1905-18.

Raynor J, Lages CS, Shehata H*, et al.* (2012) Homeostasis and function of regulatory T cells in aging. *Current Opinion in Immunology* 24:482-7.

Schenkel JM, Fraser KA, Vezys V*, et al.* (2013) Sensing and alarm function of resident memory CD8(+) T cells. *Nat Immunol* 14:509-13.

Seneschal J, Clark RA, Gehad A*, et al.* (2012) Human epidermal Langerhans cells maintain immune homeostasis in skin by activating skin resident regulatory T cells. *Immunity* 36:873-84.

Skon CN, Lee JY, Anderson KG*, et al.* (2013) Transcriptional downregulation of S1pr1 is required for the establishment of resident memory CD8+ T cells. *Nat Immunol* 14:1285-93.

Suarez-Farinas M, Haider A, Wittkowski KM (2005) "Harshlighting" small blemishes on microarrays. *BMC bioinformatics* 6:65.

Suarez-Farinas M, Tintle SJ, Shemer A*, et al.* (2011) Nonlesional atopic dermatitis skin is characterized by broad terminal differentiation defects and variable immune abnormalities. *JAllergy ClinImmunol* 127:954-64.

Tang H, Moriishi E, Okamoto S*, et al.* (2012) A community-based survey of varicella-zoster virus-specific immune responses in the elderly. *Journal of Clinical Virology* 55:46-50.

Tang VA, Rosenthal KL (2010) Intravaginal infection with herpes simplex virus type-2 (HSV-2) generates a functional effector memory T cell population that persists in the murine genital tract. *Journal of reproductive immunology* 87:39-44.

van Besouw NM, Verjans GM, Zuijderwijk JM*, et al.* (2012) Systemic varicella zoster virus reactive effector memory T-cells impaired in the elderly and in kidney transplant recipients. *Journal of medical virology* 84:2018-25.

Vukmanovic-Stejic M, Agius E, Booth N*, et al.* (2008) The kinetics of CD4Foxp3 T cell accumulation during a human cutaneous antigen-specific memory response in vivo. *J ClinInvest* 118:3639-50.

Vukmanovic-Stejic M, Rustin MH, Nikolich-Zugich J*, et al.* (2011) Immune responses in the skin in old age. *CurrOpinImmunol* 23:525-31.

Vukmanovic-Stejic M, Sandhu D, Sobande TO*, et al.* (2013) Varicella Zoster-Specific CD4+Foxp3+ T Cells Accumulate after Cutaneous Antigen Challenge in Humans. *J Immunol* 190:977-86.

Vukmanovic-Stejic M, Zhang Y, Cook JE*, et al.* (2006) Human CD4+ CD25hi Foxp3+ regulatory T cells are derived by rapid turnover of memory populations in vivo. *JClinInvest* 116:2423-33.

Wang CQF, Akalu YT, Suarez-Farinas M*, et al.* (2013) IL-17 and TNF Synergistically Modulate Cytokine Expression while Suppressing Melanogenesis: Potential Relevance to Psoriasis. *The Journal of investigative dermatology* 133:2741-52.

Weinberg A, Lazar AA, Zerbe GO*, et al.* (2010) Influence of age and nature of primary infection on varicella-zoster virus-specific cell-mediated immune responses. *The Journal of infectious diseases* 201:1024-30.

Weinberg A, Levin MJ (2010) VZV T cell-mediated immunity. *CurrTopMicrobiolImmunol* 342:341-57.

Weinberg A, Zhang JH, Oxman MN*, et al.* (2009) Varicella-zoster virus-specific immune responses to herpes zoster in elderly participants in a trial of a clinically effective zoster vaccine. *The Journal of infectious diseases* 200:1068-77.

Wherry EJ (2011) T cell exhaustion. *Nat Immunol* 12:492-9.

Wu Z, Irizarry RA (2004) Preprocessing of oligonucleotide array data. *Nature biotechnology* 22:656-8; author reply 8.

Zaba LC, Fuentes-Duculan J, Steinman RM*, et al.* (2007) Normal human dermis contains distinct populations of CD11c+BDCA-1+ dendritic cells and CD163+FXIIIA+ macrophages. *J ClinInvest* 117:2517-25.

Zaba LC, Krueger JG, Lowes MA (2008) Resident and "Inflammatory" Dendritic Cells in Human Skin. *J Invest Dermatol* 129:79-88.

Zajac AJ, Blattman JN, Murali-Krishna K*, et al.* (1998) Viral Immune Evasion Due to Persistence of Activated T Cells Without Effector Function. *The Journal of Experimental Medicine* 188:2205-13.

Zhu J, Peng T, Johnston C*, et al.* (2013) Immune surveillance by CD8alphaalpha+ skin-resident T cells in human herpes virus infection. *Nature* 497:494-7.

Cell type	Marker used	Range and mean (young)	Range and mean (old)	different
T cells	CD3	44-201, 131.8	91-291, 160.6	no
CD4+ T cells	CD4	66-145, 93.4	45-159, 103	no
CD8+ T cells	CD8	11-74, 41.6	24-110, 52,2	no
Tregs	Foxp3	1-17, 11.6	17-50, 32.8	0.0095
Dendritic cells	CD11c	46-105, 73.5	33-83, 52.75	no
Macrophages	CD163	95-326, 192.8	199-390, 278.2	no
PDC	BDCA3	18-33, 27.4	13-41, 25.75	no

Table 1. Numbers of different cell populations is normal skin

Figure Legends

Figure 1. Effect of age on circulating VZV specific CD4$^+$ T cells. (A) FACS analysis of intracellular IFN-γ staining following overnight stimulation with VZV viral lysate in the presence of brefeldin A. Representative dot plots of the CD4$^{\pm}$ IFN-γ response from young and old donors are shown and unstimulated control. Cumulative data for all donors are plotted as increasing age (years) on the *x* axis against the percentage of antigen specific IFN-γ$^+$ CD4$^+$ T cells. Line of best fit was generated by linear regression and the correlation assessed by Spearman rank correlation. (B) PBMC were stimulated with a range of doses of VZV lysate and cell proliferation measured on day 7. (C) PBMCs from young and old individuals were stimulated with VZV lysate for 72 hours and then stained for the expression of Ki67, CD4 and CD8 and analysed by FACS. Data are expressed as % of CD4$^+$ or CD8$^+$ T cells expressing Ki67 above background (unstimulated PBMC) (n=20 young and old, horizontal line represents the mean). (D) The number of antigen specific CD4$^+$ cells was also determined by class II tetramer staining. PBMC were stained with HLA-DRB1*1501 restricted IE63 tetramer and with CLIP control (Jones *et al.*, 2007; Vukmanovic-Stejic *et al.*, 2013). Each data point represents one individual (n=5 young and old individuals, mean and SEM are indicated).

Figure 2. Effect of age on the skin resident populations and gene expression profiles. Punch biopsies (5 mm) were collected from normal skin of healthy young (<40 years old) and old (>70 years old) volunteers. (A) Sections were stained to detect CD4, CD8, CD3, CD163, CD11c and Foxp3 (scale bar= 100μm). Cell numbers were expressed as the mean absolute number of cells counted within the section. The frequency of Foxp3$^+$CD4$^+$ cells was confirmed by 3 colour IF staining (Dapi- blue, CD4- green, Foxp3- red, scale bar=10μm). (B) Graph shows numbers of different cell populations in young and old skin (n=5-7 young

and old). Biopsies were collected following intradermal challenge with VZV antigen and stained for CD4 and Foxp3. Numbers of cells were counted in perivascular infiltrates (average of 5 largest perivascular infiltrates (PV) counted). Graph shows an inverse correlation between the proportion of $Foxp3^+$ cells within CD4 population and a size of the cellular infiltrate (C) (filled circles-young, open circles- old). (D) Unsupervised clustering of the skin samples from young (labels in red) and old (labels in blue) individuals based on the expression profiles using Affymetrix HG U133 Plus 2.0 arrays.

Figure 3. Effect of age on the phenotype and function of skin resident T cells. 5 mm punch biopsies and peripheral blood samples were collected from n=31 young and n=23 old donors. (A) Representative FACS histograms showing *ex vivo* CD69 expression in $CD4^+$ T cells in skin compared to the blood. Comparison of percentages of PD-1 expressing cells $CD4^+$ or $CD8^+$ T cells between skin and blood of the same donors ($p<0.001$ Wilcoxon paired test). (B) Cumulative data showing percentages of CD69 expressing cells amongst blood and skin derived $CD4^+$ T cells, stratified by donor age. Spearman correlation was used to calculate significance and deviation from zero. (C) Skin cells and PBMC were stained with CD4, CD45RA and CD27 to identify 4 differentiation subsets. Representative FACS staining of PBMC (top panels) and skin derived cells (bottom panels) from young and old donors, is shown gated on the $CD3^+CD4^+$ cells. (D) Bar chart shows cumulative data for in young and old individuals. Statistical analysis of blood and skin populations was performed using a paired t-test and p-values are indicated where relevant. (E) Skin derived leukocytes were stimulated for 5 hours with PMA and ionomycin in the presence of brefeldin A and stained for CD4, IFN-γ, IL-2, TNF-α and IL-22. Representative dot plots are shown, gated on $CD4^+$ cells (NS, non stimulated; PMA+Iono, PMA and ionomycin). (F) Graphs show % of $CD4^+$ cells staining positive for a particular cytokine (n=5-7 young and old for each cytokine).

Figure 4. Frequency of VZV specific $CD4^+$ T cells is higher in the skin compared to blood and is not affected by age. 5 mm punch biopsies and peripheral blood samples were collected from healthy young and old volunteers. Skin cells and PBMC were stimulated with VZV lysate overnight and stained for intracellular cytokines- IL-2, IFN-γ and TNF-α. (A) Representative dot plots of the $CD4^+$ IFN-γ and TNF-α response from young and old donors are shown. (B) Graph shows comparison of the frequency of cytokine secreting cells between PBMC and skin samples (n=9 old and 15 young, p=0.001 Wilcoxon paired test) each symbol represents a different individual. (C) Graph shows frequency of IFN-γ, IL-2 and TNF-α secreting VZV specific cells in young and old individuals (n≥8 young and old depending on cytokine). (D) In HLA-$DR15^+$ donors PBMC and skin derived cells were stained with HLA-DRB1*1501 restricted IE63 tetramer. Representative FACS staining is shown on the left. Bar graph represents cumulative data (n=6 young and 5 old individuals, mean and SE and p values are indicated, Wilcoxon paired test). (E) The phenotype of skin resident VZV specific IFN-γ^+ CD4 T cells was compared between young (n=12) and old individuals (n=7).

Figure 5. *Ex vivo* PD-1 expression in skin and blood derived $CD4^+$ and $CD8^+$ T cells.
PD-1 expression was measured by FACS in PBMCs or collagenase digested skin cells derived from healthy individuals (n=34, age range 19-89). (A) Representative FACS histograms showing *ex vivo* PD-1 expression in $CD4^+$ and $CD8^+$ T cells in skin compared to the blood. (B) Comparison of percentages of PD-1 expressing cells amongst total $CD4^+$ or $CD8^+$ T cells between skin and blood of the same donors ($p<0.001$ Wilcoxon paired test). (C) Cumulative data showing percentages of PD-1 expressing cells amongst blood and skin derived $CD4^+$ T cells, stratified by donor age. Spearman correlation was used to calculate significance and deviation from zero (* $p>0.05$).

a

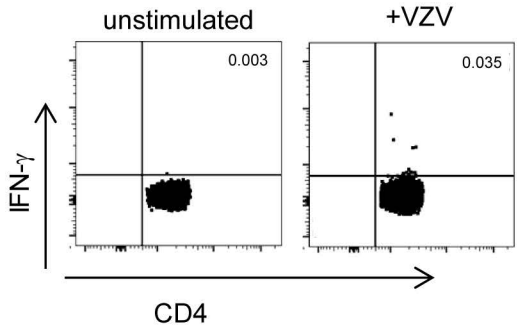
unstimulated
+VZV
0.003
0.035
IFN-γ
CD4

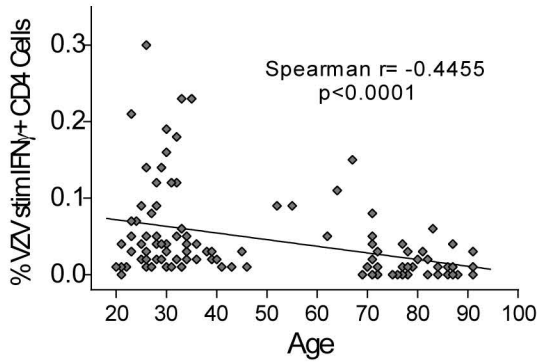
Spearman r= -0.4455
p<0.0001
% VZV stim IFNγ+ CD4 Cells
Age

b

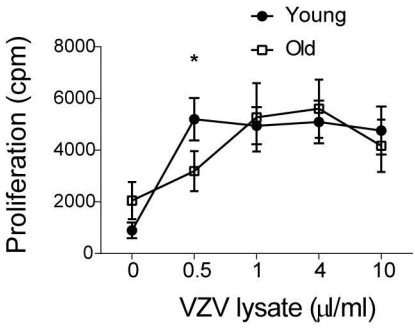
Young
Old
Proliferation (cpm)
VZV lysate (μl/ml)

c

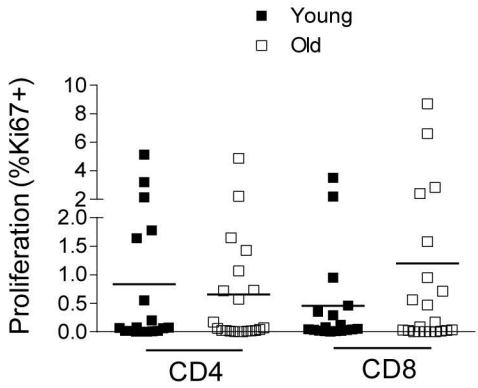
Young
Old
Proliferation (%Ki67+)
CD4
CD8

d

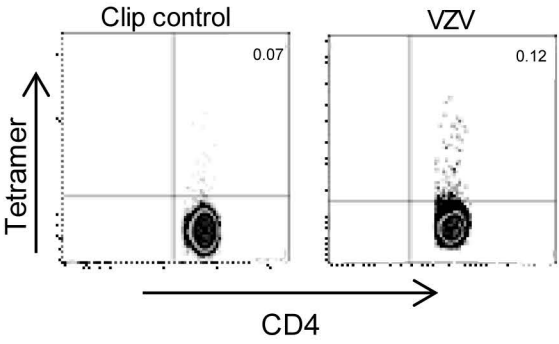
Clip control
VZV
0.07
0.12
Tetramer
CD4

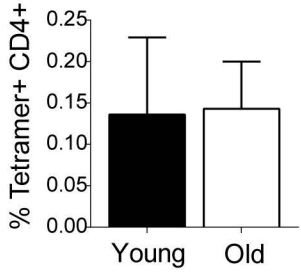
% Tetramer+ CD4+
Young
Old

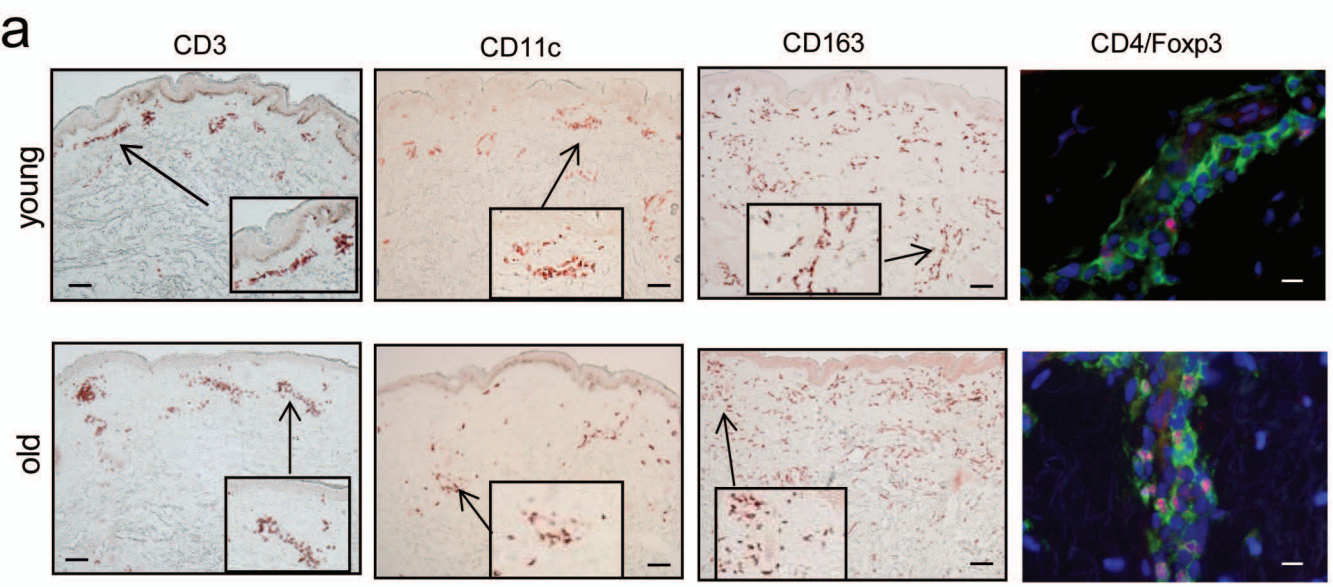
a
CD3
CD11c
CD163
CD4/Foxp3
young
old

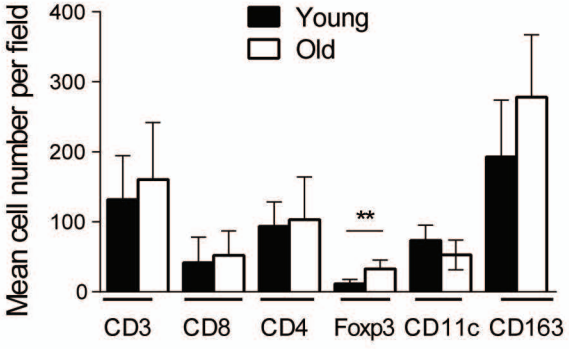
b
Young
Old
Mean cell number per field
400
300
200
100
0
**
CD3
CD8
CD4
Foxp3
CD11c
CD163

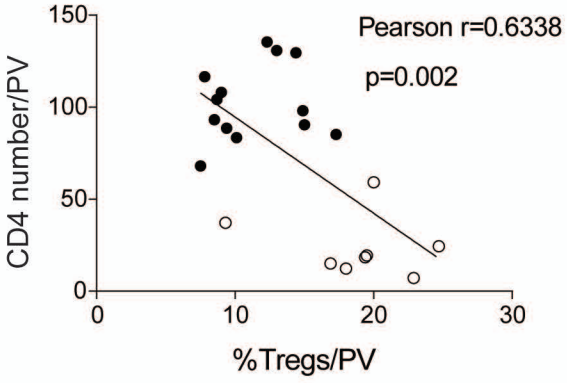
c
Pearson r=0.6338
p=0.002
CD4 number/PV
150
100
50
0
0
10
20
30
%Tregs/PV

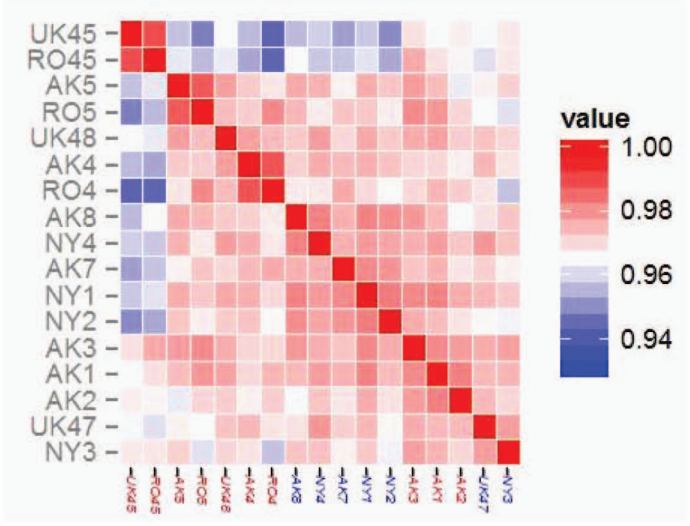
d
UK45
RO45
AK5
RO5
UK48
AK4
RO4
AK8
NY4
AK7
NY1
NY2
AK3
AK1
AK2
UK47
NY3
value
1.00
0.98
0.96
0.94

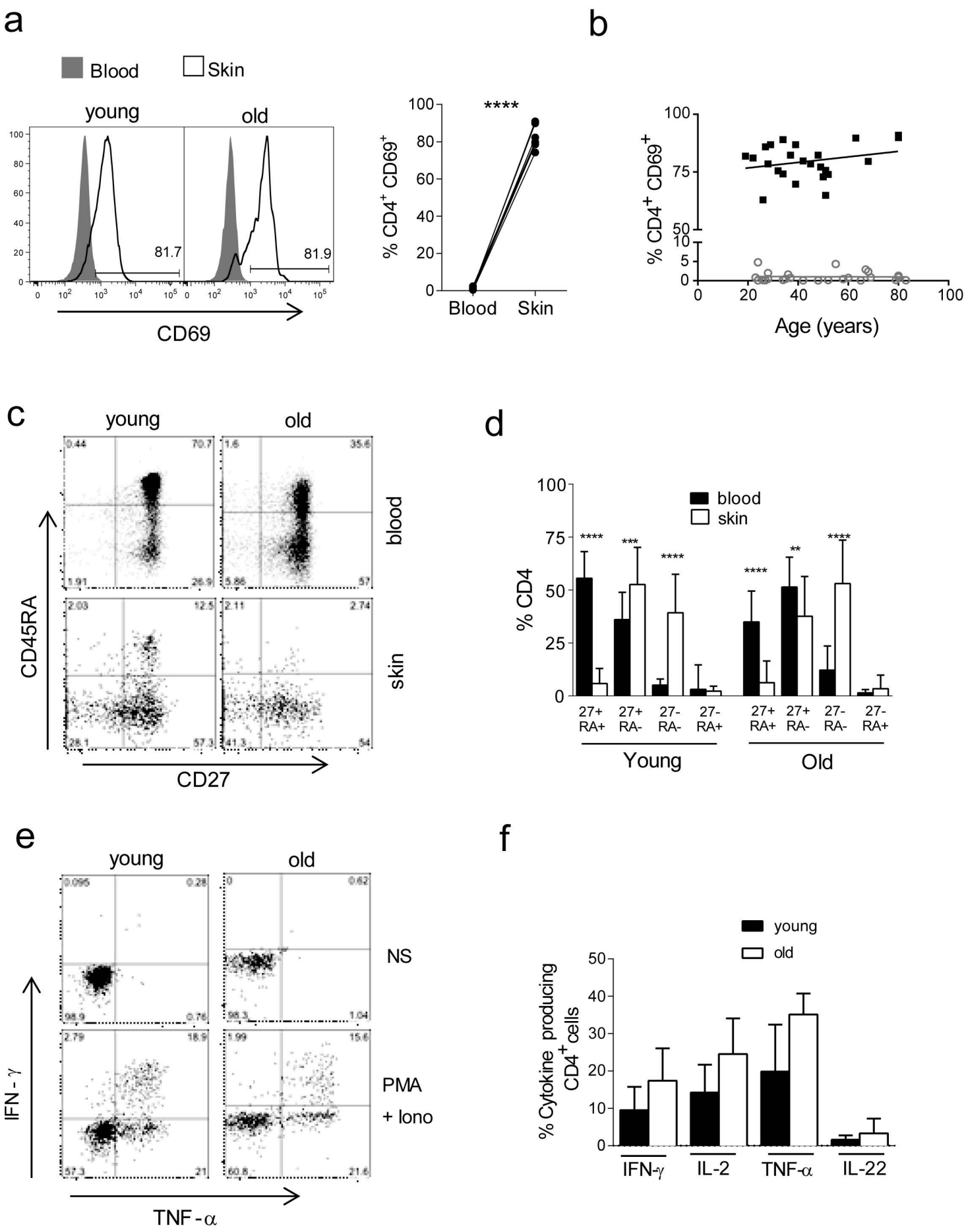
a
Blood
Skin
young
old
81.7
81.9
CD69
****
% CD4+ CD69+
Blood
Skin
b
% CD4+ CD69+
Age (years)
c
young
old
blood
skin
CD45RA
CD27
d
blood
skin
% CD4
****
***
****
****
**
****
27+ RA+
27+ RA-
27- RA-
27- RA+
Young
Old
e
young
old
NS
PMA + Iono
IFN - γ
TNF - α
f
young
old
% Cytokine producing CD4+ cells
IFN-γ
IL-2
TNF-α
IL-22

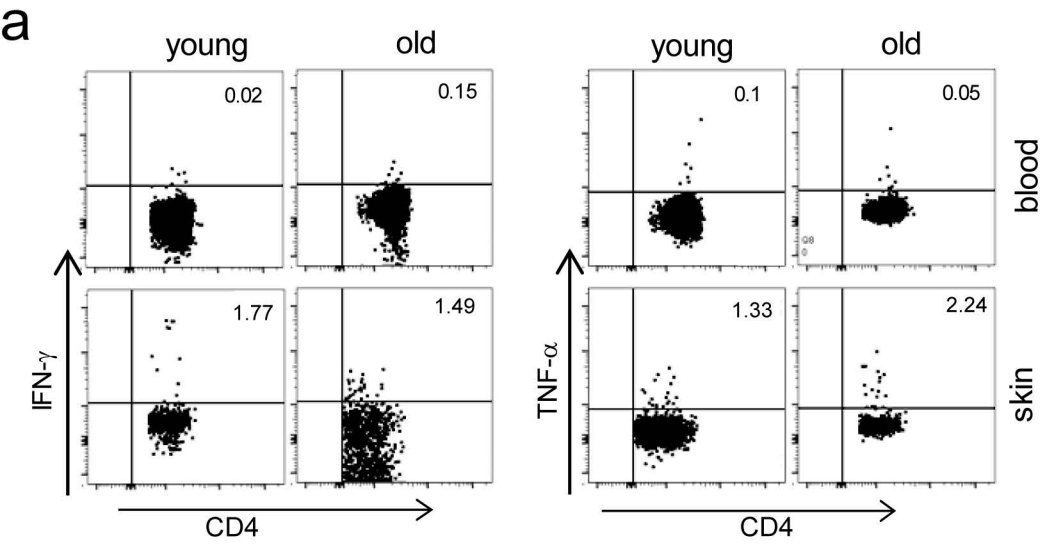
a
young
old
young
old
0.02
0.15
0.1
0.05
blood
1.77
1.49
1.33
2.24
skin
IFN-γ
TNF-α
CD4
CD4

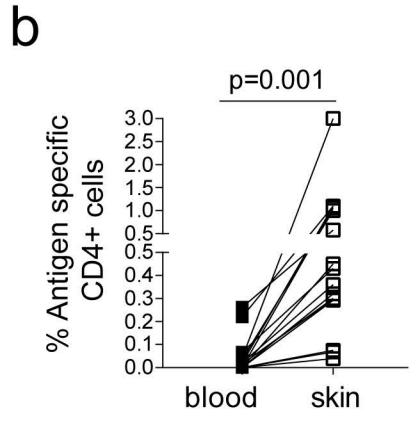
b
p=0.001
% Antigen specific CD4+ cells
blood
skin

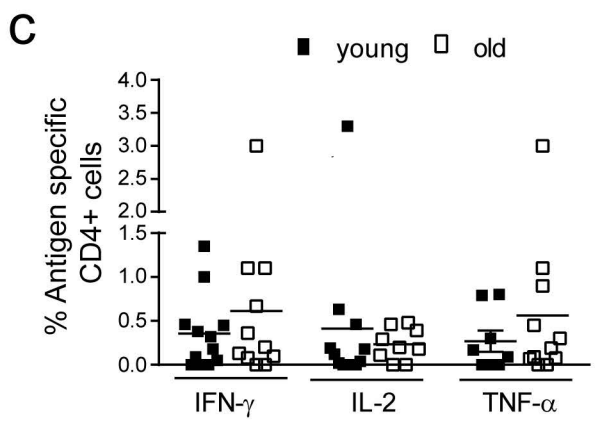
c
young
old
% Antigen specific CD4+ cells
IFN-γ
IL-2
TNF-α

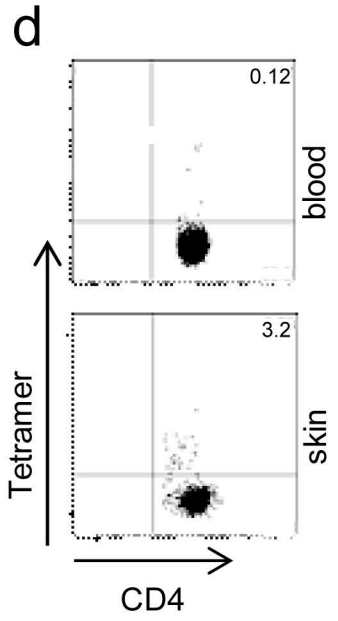
d
0.12
blood
3.2
skin
Tetramer
CD4

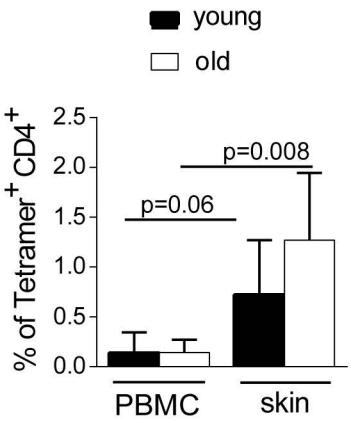
young
old
% of Tetramer+ CD4+
p=0.06
p=0.008
PBMC
skin

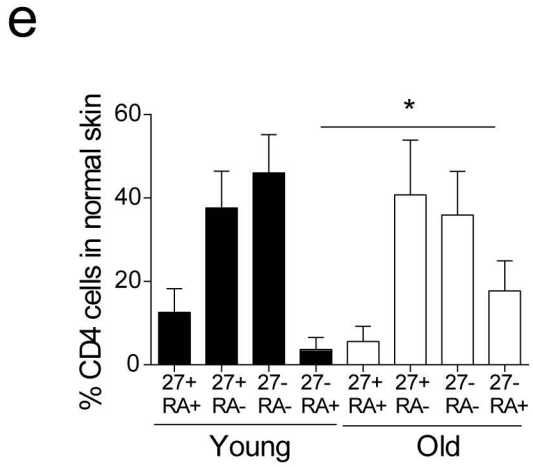
e
*
% CD4 cells in normal skin
27+ RA+
27+ RA-
27- RA-
27- RA+
27+ RA+
27+ RA-
27- RA-
27- RA+
Young
Old

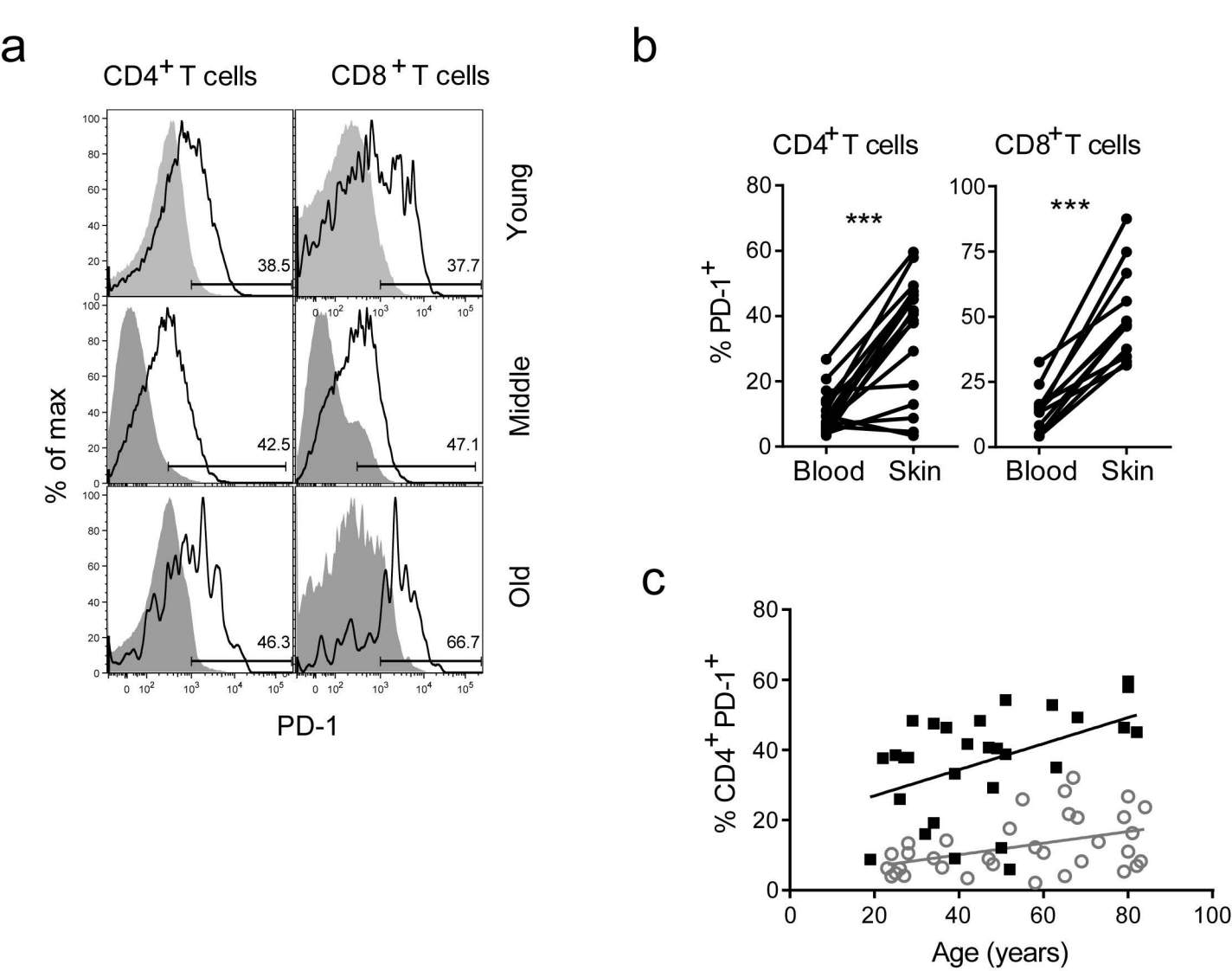
a
CD4+ T cells
CD8+ T cells
Young
Middle
Old
38.5
37.7
42.5
47.1
46.3
66.7
% of max
PD-1
b
CD4+ T cells
CD8+ T cells
% PD-1+
***
***
Blood
Skin
Blood
Skin
c
% CD4+ PD-1+
Age (years)

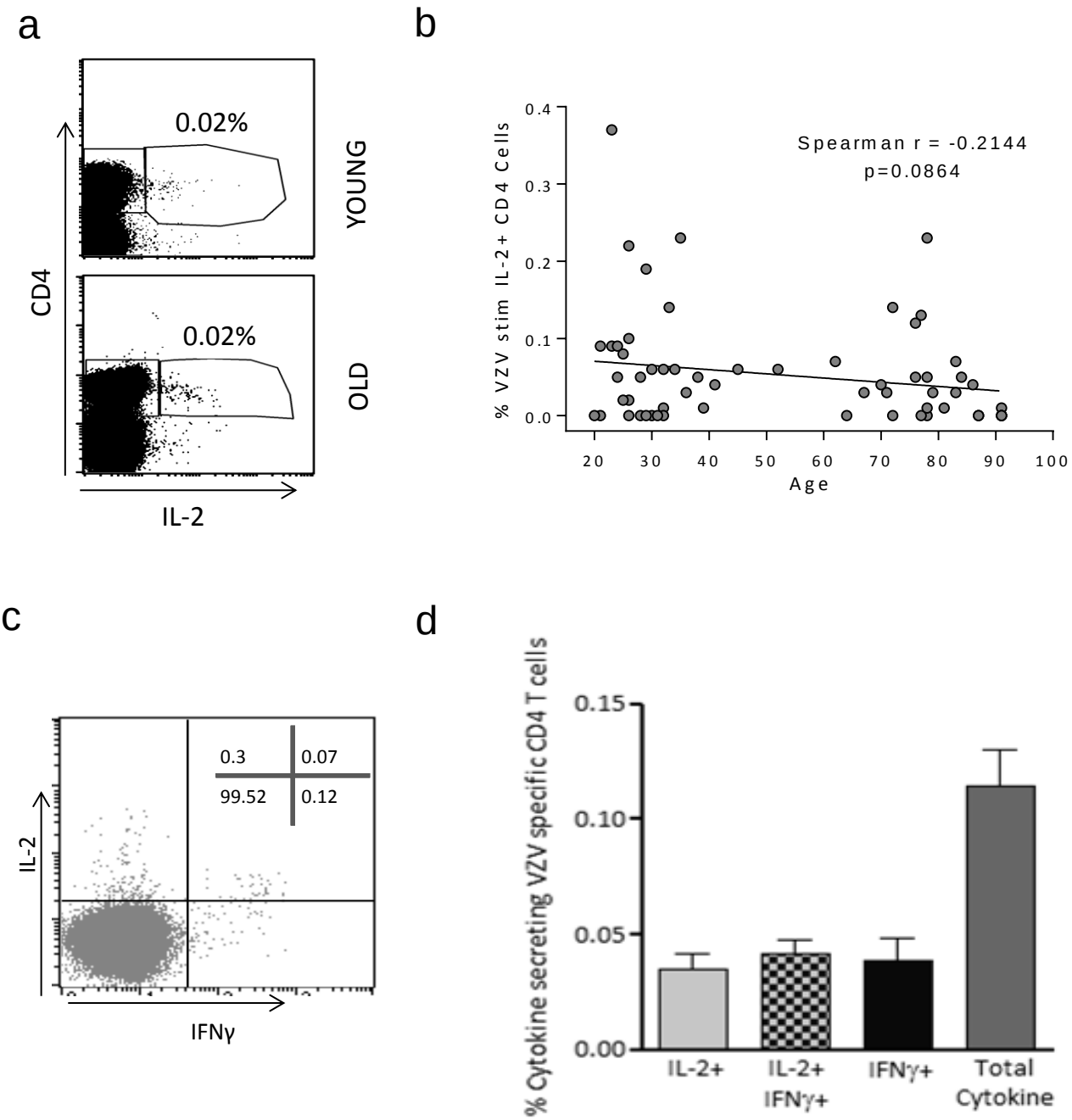

Supplementary Figure 1.The effect of age on IL-2$^+$VZV specific cells. PBMC were stimulated with VZV lysate overnight in the presence of brefeldin A, stained for IFN-γ, IL-2 and CD4 and analysed by flow cytometry. (A) Representative dot plots for IL-2 secretion in young and old. (B) Correlation with age. (C) A representative dot plot shows the distribution of IL-2 and IFN-γ secretion of gated CD4$^+$ T cells in response to VZV stimulation. (D) A bar chart summarising the percentage of CD4$^+$ T cells which secreted IL-2 alone (IL-2$^+$), IL-2 and IFN-γ (IL-2$^+$IFN-γ$^+$) or IFN-γ alone (IFN-γ$^+$) in response to VZV stimulation in 67 donors. There was no significant difference in the proportion of IL-2 or IFN-γ secreting cells using Kruskal-Wallis analysis of variance test.

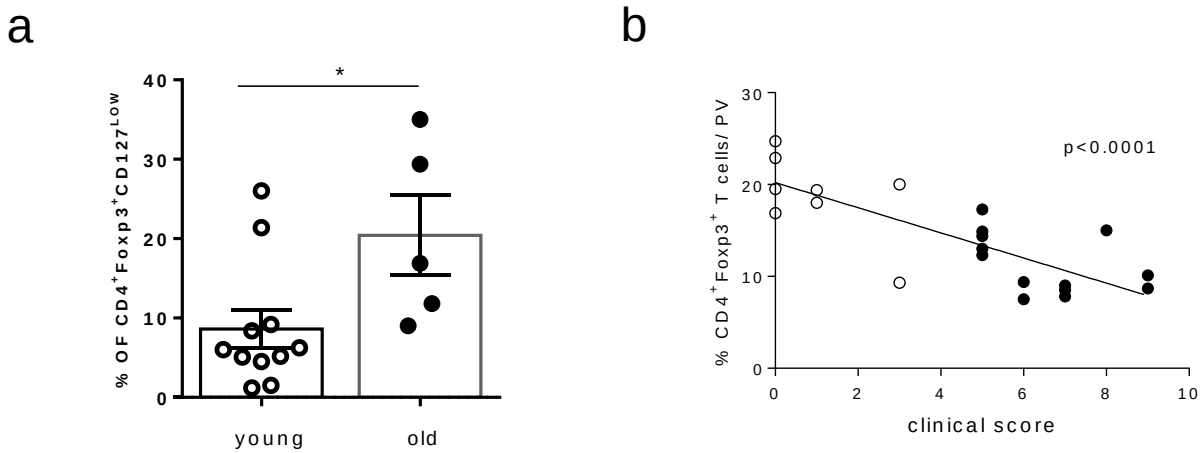

Supplementary Figure 2.The effect of age on CD4+Foxp3+ regulatory T cells in the skin. (A) PBMC and skin derived cellos were stained with CD4, Foxp3, CD127 and CD25 to enumerate the proportion of regulatory T cells in different age groups. Bars represent Mean and SEM for each age group, individual subjects are represented as separate data points. p=0.015, unpaired t-test (B) 5mm punch biopsies were collected following intradermal challenge with VZV antigen and stained for CD4 and Foxp3. Numbers of cells were counted in perivascular infiltrates (plotted as average of 5 largest perivascular infiltrates (PV) counted). Graph shows an inverse correlation between the proportion of $Foxp3^{+}$ cells within CD4 population and the clinical score (filled circles-young, open circles- old)

a

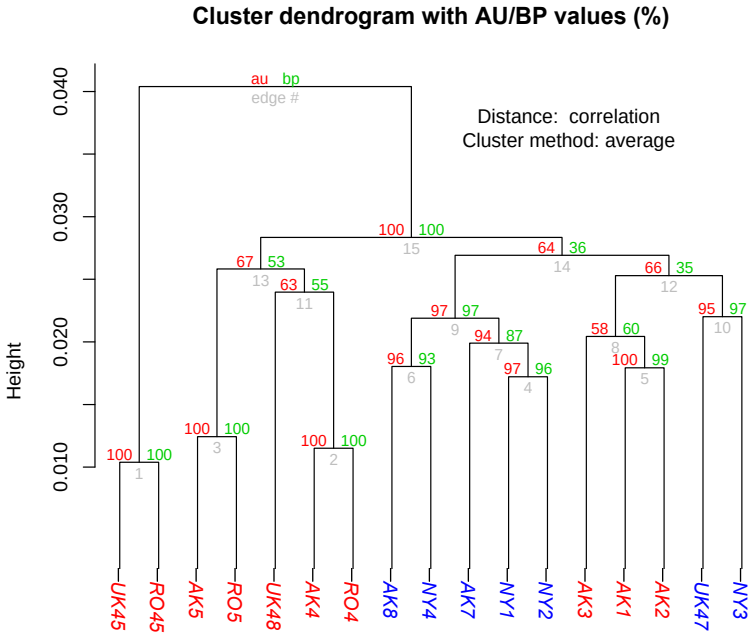

b

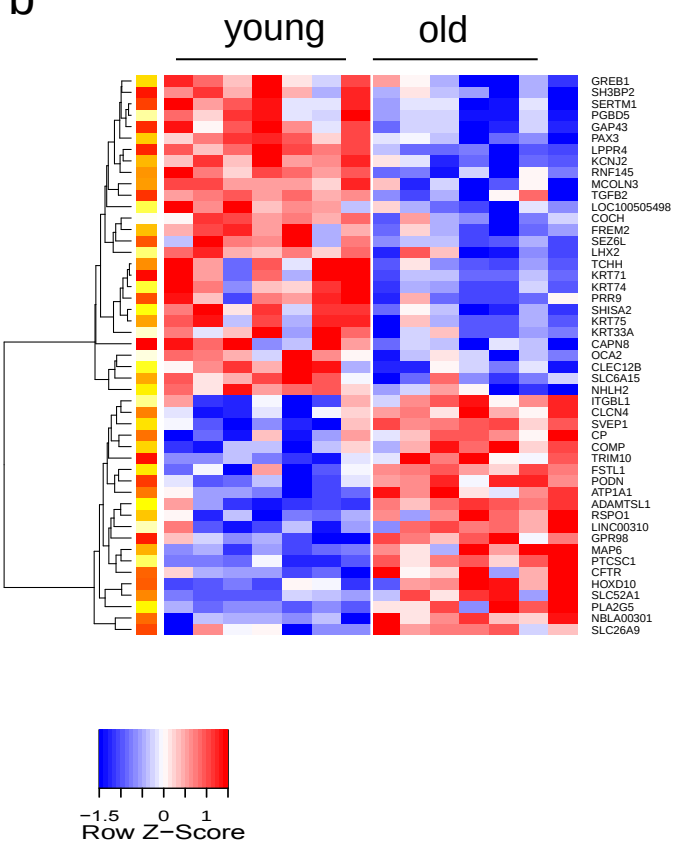

c

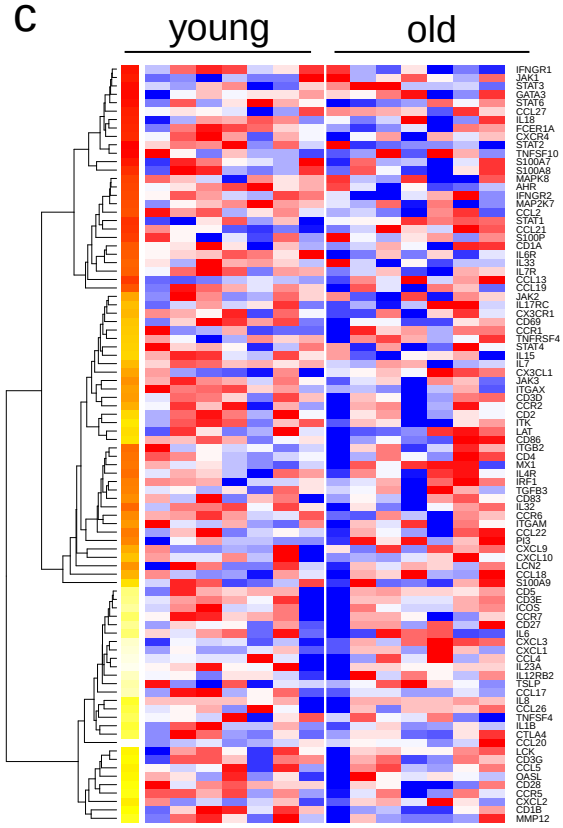

Supplementary Fig 3

d

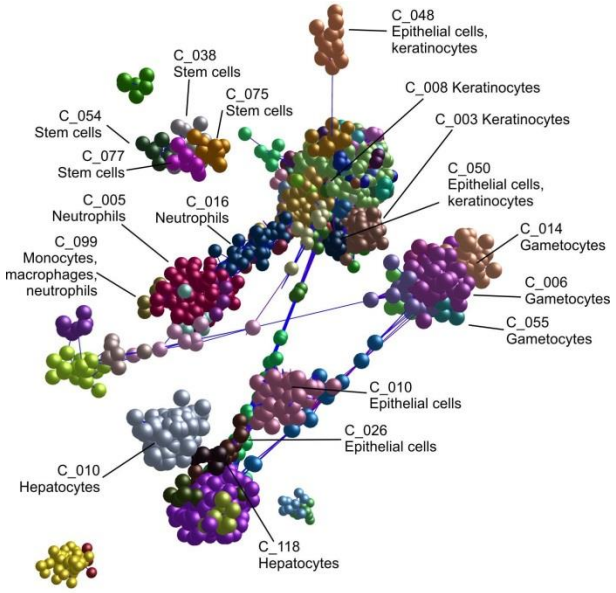

e

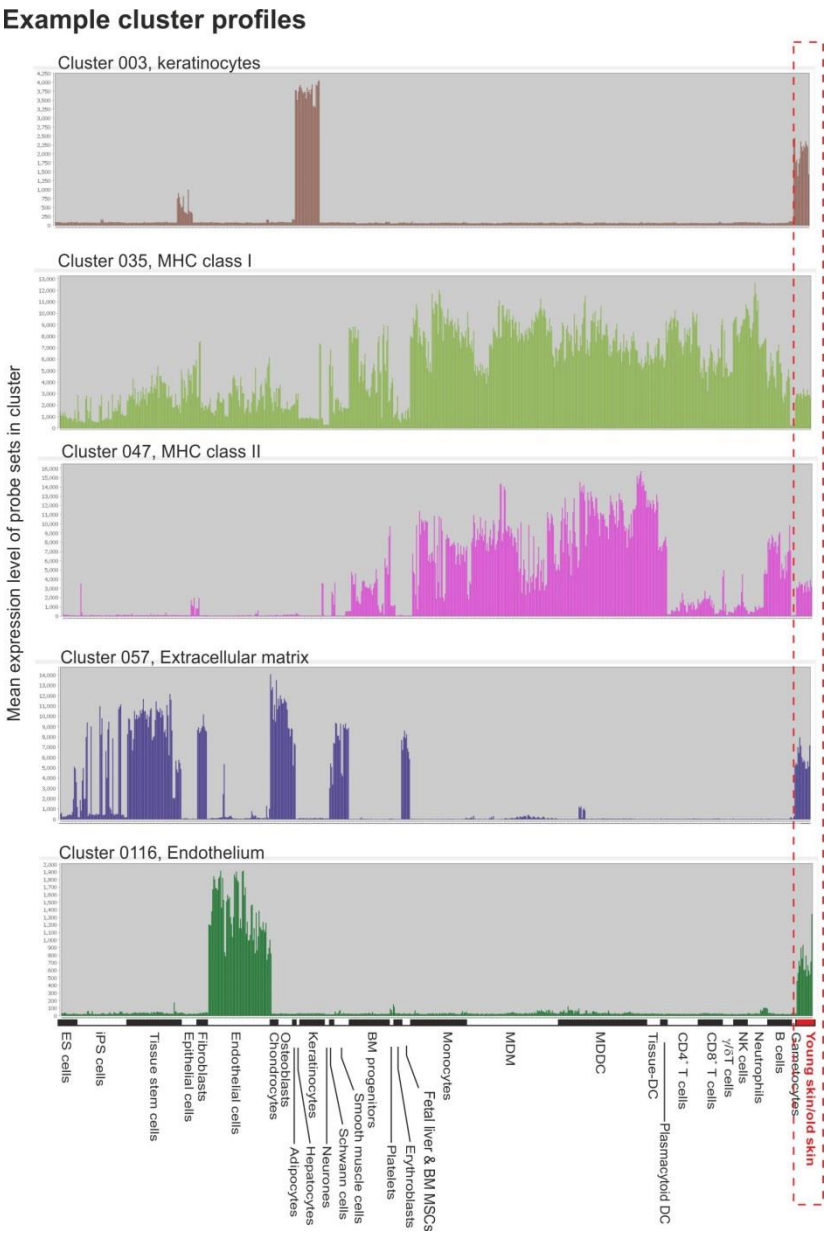

Supplementary Fig 3

Supplementary Figure 3. Transcriptomic analysis of young and old normal skin. (A) Dendogram showing the unsupervised clustering of the skin samples using the expression profiles. Simulations were run are to determine how robust the clusters to variations in the data. Clusters with high probabilities indicates stables cluster and replications from the same patient clustered together in 100% of the bootstrapping samples (eg AK5 and RO5, AK4 and RO4, UK45 and RO45). Overall no structure was identified where stable clusters were found with a pattern differentiating between young and old (indicated by blue and red color of sample ID). Similar dendograms were obtained when different agglomeration procedures where used. (B) Heatmap shows the relative expression of differentially expressed genes between young and old skin at FCH>2 and FDR>0.2. (C) Heatmap shows the relative expression of immune genes (manually curated by our lab and extensively used (38) showing no discernible pattern of expression differentiating skin from young and old healthy individuals. For each gene, only the probeset with the largest average expression is shown. (D) Network analysis of the human skin-punch biopsies and 745 primary cell gene-expression data sets using the tool BioLayout Express3D. This analysis enabled the visualization of genes within a cluster across the entire data collection. Genes with similar expression profiles are clustered together within the same region of the network graph. Nodes represent transcripts (probe sets) and the edges represent correlations between individual expression profiles above $r = 0.90$. The nodes are coloured according to the cluster to which they have been assigned. The positions of representative clusters are annotated. (E) Young and old skin samples shared similar gene cluster expression profiles. Five representative clusters derived from the network graph are shown and their mean probe set expression profiles across all data sets. The boxed area surrounded by a red line indicates the location of the young and old skin data sets. Cluster 003 contained genes that are highly expressed by keratinocytes, and cluster 116 contained endothelium-related genes. Cluster 035 contained genes encoding MHC class I, whereas cluster 047 contained genes encoding MHC class II. Cluster 057 was enriched in extracellular matrix-related genes. The genes in these clusters were expressed at similar levels across all of the young and old skin samples. ES cells, embryonic stem cells; iPS cells, induced pluoripotent stem cells; BM, bone marrow; MSC, mesenchymal stem cells; MDM, monocyte-derived macrophage; MDDC, monocyte-derived dendritic cells; NK, natural killer cells.

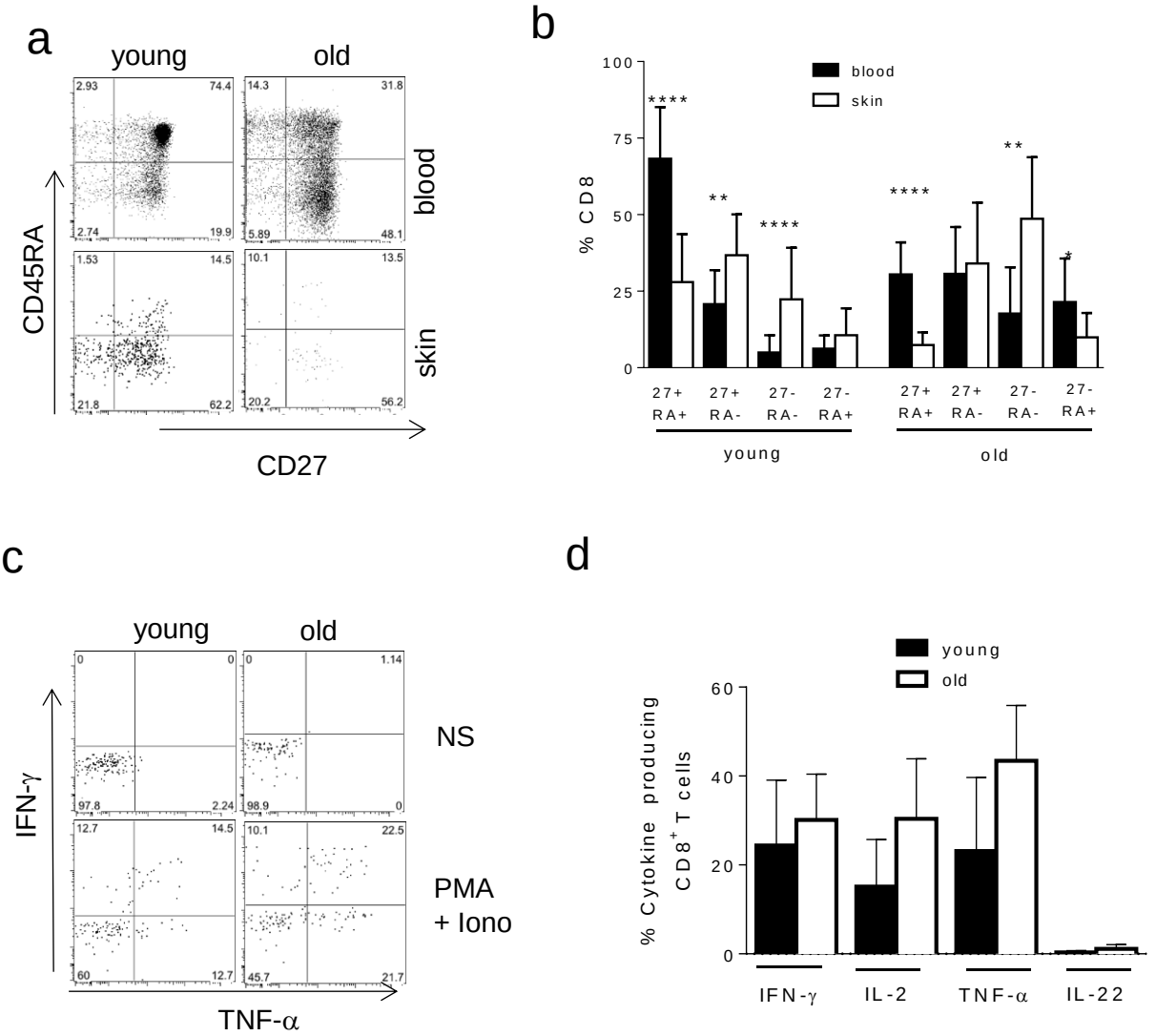

Supplementary Figure 4. Effect of age on the phenotype and function of skin resident CD8+ T cells. 5 mm punch biopsies and peripheral blood samples were collected from n=31 young and n=23 old donors. Following overnight digestion of biopsies, skin cells and PBMC were stained with CD8, CD45RA and CD27 to identify 4 differentiation subsets. Representative FACS staining of PBMC (top panels) and skin derived cells (bottom panels) from young and old donors, is shown gated on the $CD3^{+}CD8^{+}$ cells. (B) Bar chart shows cumulative data for in young and old individuals. Statistical analysis of blood and skin populations was performed using a paired t-test and p-values are indicated where relevant. (C) Skin derived leukocytes were stimulated for 5 hours with PMA and ionomycin in the presence of brefeldin A and stained for CD8, IFN-γ, IL-2, TNF-α and IL-22. Representative dot plots are shown, gated on $CD8^{+}$ cells (NS, non stimulated; PMA+Iono, PMA and ionomycin). (D) Graphs show % of $CD8^{+}$ cells staining positive for a particular cytokine (n=5-7 young and old for each cytokine).

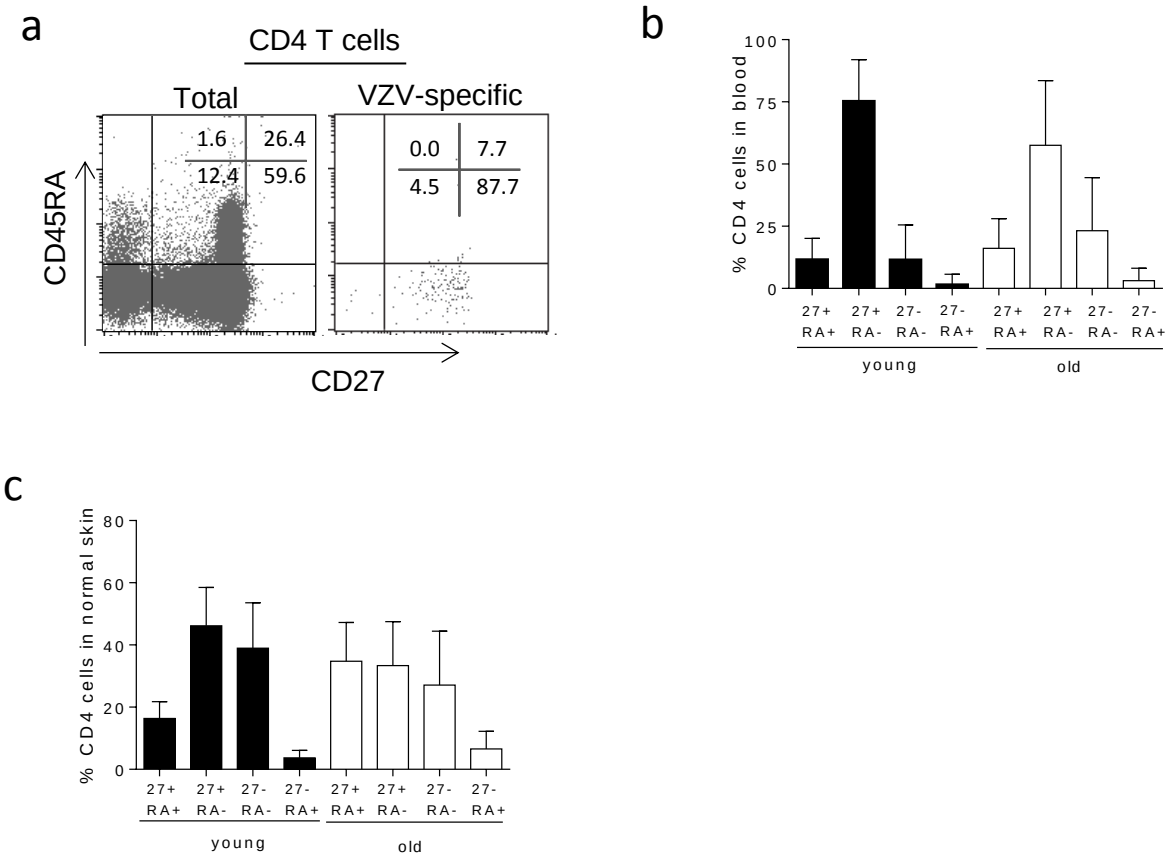

Supplementary figure 5. VZV specific cells have a central memory phenotype and there is no significant difference between young and old. PBMCs were stained with CD4, CD27, CD45RA and intracellular IFN-γ antibodies following overnight stimulation with VZV lysate in the presence of brefeldin A. Representative dot plots showing the CD27 and CD45RA phenotype of VZV specific $CD4^+$ T cells secreting IFN-γ (A) compared to the total $CD4^+$ T cell population are shown for young and old individuals. (B) Graph shows the phenotype of circulating VZV specific (IFN-γ^+) cells in young and old donors (n= 45 young, 24 old). (C) Phenotype of VZV-specific skin resident T cells. In HLA-$DR15^+$ donors skin derived cells were stained with HLA-DRB1*1501 restricted IE63 tetramer and the phenotype was compared based on CD45RA and CD27 expression.

Supplementary Table 1. List of probesets and genes within the clusters of interest derived from the network graph. Gene expression profiles in the young and aged skin samples were compared with that of a large collection of microarray data sets from distinct human primary cell populations (745 individual data sets,) using the bioinformatics tool Biolayout Express3D. 11,914 probe sets (genes) were clustered together using a Pearson correlation threshold of r=0.90 and Markov clustering algorithm of 2.2 into 140 clusters containing $\geq$ 5ptrobe sets. The contents of selected clusters of interest derived from the network graph are presented.

Name	Symbol	Description	FC (Old v. Young)
A2ML1;1553505_at	A2ML1	alpha-2-macroglobulin-like 1	1.31
A2ML1;1564307_a_at	A2ML1	alpha-2-macroglobulin-like 1	1.51
AADACL2;240420_at	AADACL2	arylacetamide deacetylase-like 2	1.07
ABCA12;215465_at	ABCA12	ATP-binding cassette, sub-family A (ABC1), n	1.70
ACER1;1553929_at	ACER1	alkaline ceramidase 1	1.30
AKR1B10;206561_s_at	AKR1B10	aldo-keto reductase family 1, member B10 (	0.98
ALDH3B2;204941_s_at	ALDH3B2	aldehyde dehydrogenase 3 family, member	0.94
ALOX12B;207381_at	ALOX12B	arachidonate 12-lipoxygenase, 12R type	1.51
ALOXE3;207708_at	ALOXE3	arachidonate lipoxygenase 3	1.46
ALOXE3;222383_s_at	ALOXE3	arachidonate lipoxygenase 3	1.48
ALS2CL;222333_at	ALS2CL	ALS2 C-terminal like	1.09
ANKRD13C;1556361_s_at	ANKRD13C	ankyrin repeat domain 13C	0.96
ANXA9;210085_s_at	ANXA9	annexin A9	1.39
ANXA9;211712_s_at	ANXA9	annexin A9	1.34
ARSF;214490_at	ARSF	arylsulfatase F	1.47
ASPRV1;235514_at	ASPRV1	aspartic peptidase, retroviral-like 1	1.44
ATP10B;214070_s_at	ATP10B	ATPase, class V, type 10B	1.21
ATP6V1C2;1552532_a_at	ATP6V1C2	ATPase, H+ transporting, lysosomal 42kDa, \	1.05
ATP6V1C2;1553989_a_at	ATP6V1C2	ATPase, H+ transporting, lysosomal 42kDa, \	1.03
BLMH;202179_at	BLMH	bleomycin hydrolase	1.41
BNIPL;1553072_at	BNIPL	BCL2/adenovirus E1B 19kD interacting prote	0.90
BPIL2;1555773_at	BPIL2	bactericidal/permeability-increasing protein	1.20
C10orf99;227736_at	C10orf99	chromosome 10 open reading frame 99	1.75
C12orf29;228378_at	C12orf29	chromosome 12 open reading frame 29	1.15
C1orf116;228865_at	C1orf116	chromosome 1 open reading frame 116	1.30
C1orf46;216935_at	C1orf46	chromosome 1 open reading frame 46	1.49
C1orf68;217087_at	C1orf68	chromosome 1 open reading frame 68	1.18
C9orf169;1569144_a_at	C9orf169	chromosome 9 open reading frame 169	1.43
CALML3;210020_x_at	CALML3	calmodulin-like 3	0.87
CALML5;220414_at	CALML5	calmodulin-like 5	1.32
CARD18;231733_at	CARD18	caspase recruitment domain family, membe	1.36
CASP14;231722_at	CASP14	caspase 14, apoptosis-related cysteine pepti	1.37
CDS1;205709_s_at	CDS1	CDP-diacylglycerol synthase (phosphatidate	1.04
CDS1;226187_at	CDS1	CDP-diacylglycerol synthase (phosphatidate	1.11
CDSN;206192_at	CDSN	corneodesmosin	1.39
CDSN;206193_s_at	CDSN	corneodesmosin	1.68
CENPT;218148_at	CENPT	centromere protein T	0.98
CHMP4C;226803_at	CHMP4C	chromatin modifying protein 4C	1.17
CLCA2;206164_at	CLCA2	chloride channel accessory 2	1.00
CLCA2;206165_s_at	CLCA2	chloride channel accessory 2	1.02
CLCA2;206166_s_at	CLCA2	chloride channel accessory 2	1.11
CLCA2;217528_at	CLCA2	chloride channel accessory 2	1.00
CLDN1;222549_at	CLDN1	claudin 1	0.99
CLTB;205172_x_at	CLTB	clathrin, light chain (Lcb)	1.10
CLTB;206284_x_at	CLTB	clathrin, light chain (Lcb)	1.11
CLTB;211043_s_at	CLTB	clathrin, light chain (Lcb)	1.04
CNFN;224329_s_at	CNFN	cornifelin	1.67
CPA4;205832_at	CPA4	carboxypeptidase A4	0.97
CRCT1;220620_at	CRCT1	cysteine-rich C-terminal 1	1.42

CST6;206595_at	CST6	cystatin E/M	0.93
CWH43;220723_s_at	CWH43	cell wall biogenesis 43 C-terminal homolog (	1.03
CWH43;220724_at	CWH43	cell wall biogenesis 43 C-terminal homolog (	1.08
CXCL14;218002_s_at	CXCL14	chemokine (C-X-C motif) ligand 14	1.10
CXCL14;222484_s_at	CXCL14	chemokine (C-X-C motif) ligand 14	1.00
CYP4F22;244692_at	CYP4F22	cytochrome P450, family 4, subfamily F, poly	1.20
D4S234E;209569_x_at	D4S234E	DNA segment on chromosome 4 (unique) 23	1.05
D4S234E;213533_at	D4S234E	DNA segment on chromosome 4 (unique) 23	1.04
DAPL1;229290_at	DAPL1	death associated protein-like 1	1.04
DEFB1;210397_at	DEFB1	defensin, beta 1	1.09
DEGS2;236496_at	DEGS2	degenerative spermatocyte homolog 2, lipid	1.12
DENND2C;233294_at	DENND2C	DENN/MADD domain containing 2C	0.93
DHRS1;213279_at	DHRS1	dehydrogenase/reductase (SDR family) mem	0.97
DIO2;203699_s_at	DIO2	deiodinase, iodothyronine, type II	0.99
DMKN;226926_at	DMKN	dermokine	1.10
DNASE1L2;207192_at	DNASE1L2	deoxyribonuclease I-like 2	0.87
DSC1;207324_s_at	DSC1	desmocollin 1	1.03
DSG1;206642_at	DSG1	desmoglein 1	1.02
DSG3;205595_at	DSG3	desmoglein 3 (pemphigus vulgaris antigen)	0.97
DSG3;235075_at	DSG3	desmoglein 3 (pemphigus vulgaris antigen)	0.95
DUOX1;215800_at	DUOX1	dual oxidase 1	1.06
DUOXA1;1554648_a_at	DUOXA1	dual oxidase maturation factor 1	0.99
ELF5;220624_s_at	ELF5	E74-like factor 5 (ets domain transcription fa	1.00
ELF5;220625_s_at	ELF5	E74-like factor 5 (ets domain transcription fa	1.25
ELMOD1;231930_at	ELMOD1	ELMO/CED-12 domain containing 1	1.79
ELOVL4;219532_at	ELOVL4	elongation of very long chain fatty acids (FEN	1.00
EPHX3;220013_at	EPHX3	epoxide hydrolase 3	1.24
EPN3;220318_at	EPN3	epsin 3	1.17
EPN3;223895_s_at	EPN3	epsin 3	1.08
EPPK1;208156_x_at	EPPK1	epiplakin 1	1.26
EPPK1;232164_s_at	EPPK1	epiplakin 1	1.08
EPPK1;232165_at	EPPK1	epiplakin 1	1.08
EPPK1;234552_at	EPPK1	epiplakin 1	1.57
EPS8L1;218779_x_at	EPS8L1	EPS8-like 1	1.23
EPS8L1;221655_x_at	EPS8L1	EPS8-like 1	1.23
EPS8L1;221665_s_at	EPS8L1	EPS8-like 1	1.26
EPS8L1;91826_at	EPS8L1	EPS8-like 1	1.21
ESRP2;219395_at	ESRP2	epithelial splicing regulatory protein 2	1.04
ESYT3;1554912_at	ESYT3	extended synaptotagmin-like protein 3	1.20
ESYT3;239770_at	ESYT3	extended synaptotagmin-like protein 3	1.24
EVPL;204503_at	EVPL	envoplakin	1.09
EXPH5;213929_at	EXPH5	exophilin 5	0.86
EXPH5;214734_at	EXPH5	exophilin 5	0.71
FAM59A;219377_at	FAM59A	family with sequence similarity 59, member	1.07
FBXO45;225100_at	FBXO45	F-box protein 45	1.40
FCHSD1;226698_at	FCHSD1	FCH and double SH3 domains 1	1.07
FLG;215704_at	FLG	filaggrin	1.13
FLG2;1569410_at	FLG2	filaggrin family member 2	1.09
FLJ41603;227717_at	FLJ41603	FLJ41603 protein	1.10
FRMPD1;206774_at	FRMPD1	FERM and PDZ domain containing 1	1.09

GDA;224209_s_at	GDA	guanine deaminase	2.26
GDPD2;220291_at	GDPD2	glycerophosphodiester phosphodiesterase d	0.95
GDPD3;219722_s_at	GDPD3	glycerophosphodiester phosphodiesterase d	1.13
GJB2;223278_at	GJB2	gap junction protein, beta 2, 26kDa	1.04
GJB6;231771_at	GJB6	gap junction protein, beta 6, 30kDa	1.05
GLTP;219267_at	GLTP	glycolipid transfer protein	1.13
GLTP;226177_at	GLTP	glycolipid transfer protein	1.07
GPR115;1553031_at	GPR115	G protein-coupled receptor 115	1.21
GPR87;219936_s_at	GPR87	G protein-coupled receptor 87	1.17
GRHL1;1552685_a_at	GRHL1	grainyhead-like 1 (Drosophila)	1.11
GRHL1;222830_at	GRHL1	grainyhead-like 1 (Drosophila)	1.07
GRHL3;232116_at	GRHL3	grainyhead-like 3 (Drosophila)	1.40
GSDMC;234305_s_at	GSDMC	gasdermin C	0.96
GSTA4;202967_at	GSTA4	glutathione S-transferase alpha 4	1.03
HAL;206643_at	HAL	histidine ammonia-lyase	1.24
HOPX;1566140_at	HOPX	HOP homeobox	1.07
HOPX;211597_s_at	HOPX	HOP homeobox	1.16
HPGD;203913_s_at	HPGD	hydroxyprostaglandin dehydrogenase 15-(N	1.12
HPGD;203914_x_at	HPGD	hydroxyprostaglandin dehydrogenase 15-(N	1.17
HPGD;211548_s_at	HPGD	hydroxyprostaglandin dehydrogenase 15-(N	1.23
HPGD;211549_s_at	HPGD	hydroxyprostaglandin dehydrogenase 15-(N	1.05
HS3ST6;239547_at	HS3ST6	heparan sulfate (glucosamine) 3-O-sulfotran	0.88
HSPC159;219998_at	HSPC159	galectin-related protein	1.29
HSPC159;226188_at	HSPC159	galectin-related protein	1.09
HYAL4;220249_at	HYAL4	hyaluronoglucosaminidase 4	1.44
IDE;203328_x_at	IDE	insulin-degrading enzyme	1.56
IDE;217496_s_at	IDE	insulin-degrading enzyme	1.57
IFFO2;225615_at	IFFO2	intermediate filament family orphan 2	0.99
IGFL2;231148_at	IGFL2	IGF-like family member 2	0.76
IL18;206295_at	IL18	interleukin 18 (interferon-gamma-inducing f	1.06
IL1F10;224262_at	IL1F10	interleukin 1 family, member 10 (theta)	2.20
IL1F5;222223_s_at	IL1F5	interleukin 1 family, member 5 (delta)	1.51
IL1F8;231755_at	IL1F8	interleukin 1 family, member 8 (eta)	2.61
IL1F9;220322_at	IL1F9	interleukin 1 family, member 9	1.52
IL20RA;219115_s_at	IL20RA	interleukin 20 receptor, alpha	0.90
IRX4;220225_at	IRX4	iroquois homeobox 4	0.85
IVL;214599_at	IVL	involucrin	1.65
JUP;201015_s_at	JUP	junction plakoglobin	1.04
KCTD1;226245_at	KCTD1	potassium channel tetramerisation domain c	0.95
KCTD1;226246_at	KCTD1	potassium channel tetramerisation domain c	0.96
KCTD4;239787_at	KCTD4	potassium channel tetramerisation domain c	1.18
KCTD4;240512_x_at	KCTD4	potassium channel tetramerisation domain c	1.00
KLC3;1570402_at	KLC3	kinesin light chain 3	1.02
KLC3;239853_at	KLC3	kinesin light chain 3	1.02
KLK10;209792_s_at	KLK10	kallikrein-related peptidase 10	1.00
KLK10;215808_at	KLK10	kallikrein-related peptidase 10	1.10
KLK11;205470_s_at	KLK11	kallikrein-related peptidase 11	0.97
KLK5;222242_s_at	KLK5	kallikrein-related peptidase 5	1.44
KLK7;205778_at	KLK7	kallikrein-related peptidase 7	1.27
KLK7;239381_at	KLK7	kallikrein-related peptidase 7	1.06

KLK8;1552319_a_at	KLK8	kallikrein-related peptidase 8	1.17
KLK8;206125_s_at	KLK8	kallikrein-related peptidase 8	1.19
KRT1;205900_at	KRT1	keratin 1	1.05
KRT10;207023_x_at	KRT10	keratin 10	0.98
KRT10;210633_x_at	KRT10	keratin 10	0.96
KRT10;213287_s_at	KRT10	keratin 10	0.95
KRT14;209351_at	KRT14	keratin 14	0.97
KRT16;209800_at	KRT16	keratin 16	0.89
KRT17;205157_s_at	KRT17	keratin 17	0.58
KRT17;212236_x_at	KRT17	keratin 17	0.70
KRT2;207908_at	KRT2	keratin 2	1.03
KRT23;218963_s_at	KRT23	keratin 23 (histone deacetylase inducible)	1.41
KRT6A;209125_at	KRT6A	keratin 6A	0.54
KRT6B;209126_x_at	KRT6B	keratin 6B	0.82
KRT6B;213680_at	KRT6B	keratin 6B	0.80
KRT78;1553212_at	KRT78	keratin 78	1.33
KRT78;1553213_a_at	KRT78	keratin 78	1.44
KRT80;231849_at	KRT80	keratin 80	1.27
KRT9;208188_at	KRT9	keratin 9	0.73
KRTDAP;230835_at	KRTDAP	keratinocyte differentiation-associated prot	1.09
LAD1;203287_at	LAD1	ladinin 1	1.11
LAD1;216641_s_at	LAD1	ladinin 1	1.24
LASS3;1554252_a_at	LASS3	LAG1 homolog, ceramide synthase 3	1.19
LASS3;1554253_a_at	LASS3	LAG1 homolog, ceramide synthase 3	1.18
LCE1B;1560531_at	LCE1B	late cornified envelope 1B	1.24
LCE1E;1559224_at	LCE1E	late cornified envelope 1E	1.01
LCE1E;1559226_x_at	LCE1E	late cornified envelope 1E	1.01
LCE2B;207710_at	LCE2B	late cornified envelope 2B	1.19
LCE3D;224328_s_at	LCE3D	late cornified envelope 3D	2.52
LOC100130476;243871_a	LOC100130476	similar to hCG2036711	1.14
LOC284023;238096_at	LOC284023	hypothetical protein LOC284023	1.12
LOR;207720_at	LOR	loricrin	1.33
LY6D;206276_at	LY6D	lymphocyte antigen 6 complex, locus D	1.12
LY6G6C;207114_at	LY6G6C	lymphocyte antigen 6 complex, locus G6C	1.27
LYNX1;1554179_s_at	LYNX1	Ly6/neurotoxin 1	1.74
LYPD3;204952_at	LYPD3	LY6/PLAUR domain containing 3	1.14
MAP2;210015_s_at	MAP2	microtubule-associated protein 2	1.30
MBD1;241813_at	MBD1	methyl-CpG binding domain protein 1	1.08
MUC15;227238_at	MUC15	mucin 15, cell surface associated	0.97
MUC15;227241_at	MUC15	mucin 15, cell surface associated	0.95
MUCL1;1553602_at	MUCL1	mucin-like 1	0.83
MYO5B;225301_s_at	MYO5B	myosin VB	1.22
NA;1556161_a_at	NA	NA	1.99
NA;1556194_a_at	NA	NA	0.88
NA;1558687_a_at	NA	NA	1.05
NA;1570192_at	NA	NA	1.00
NA;206400_at	NA	NA	1.03
NA;208539_x_at	NA	NA	2.84
NA;214580_x_at	NA	NA	0.80
NA;217521_at	NA	NA	1.34

NA;219095_at	NA	NA	1.11
NA;227735_s_at	NA	NA	1.80
NA;228587_at	NA	NA	1.01
NA;231033_at	NA	NA	0.87
NA;236069_at	NA	NA	1.40
NA;238710_at	NA	NA	1.32
NA;239736_at	NA	NA	1.15
NA;239841_at	NA	NA	1.14
NA;242951_at	NA	NA	1.20
NA;60528_at	NA	NA	1.12
NIPAL4;230188_at	NIPAL4	NIPA-like domain containing 4	1.25
NKPD1;1560430_at	NKPD1	NTPase, KAP family P-loop domain containin	1.04
NLRP10;1553534_at	NLRP10	NLR family, pyrin domain containing 10	1.65
NLRX1;1553695_a_at	NLRX1	NLR family member X1	1.11
NLRX1;219680_at	NLRX1	NLR family member X1	1.18
OTUB2;219369_s_at	OTUB2	OTU domain, ubiquitin aldehyde binding 2	1.18
OVOL1;206604_at	OVOL1	ovo-like 1(Drosophila)	1.48
OVOL1;229396_at	OVOL1	ovo-like 1(Drosophila)	1.46
PGLYRP4;220944_at	PGLYRP4	peptidoglycan recognition protein 4	1.15
PKP1;205724_at	PKP1	plakophilin 1 (ectodermal dysplasia/skin frag	1.17
PKP1;221854_at	PKP1	plakophilin 1 (ectodermal dysplasia/skin frag	0.99
PKP3;209872_s_at	PKP3	plakophilin 3	1.04
PKP3;209873_s_at	PKP3	plakophilin 3	1.02
PNLIPRP3;1558846_at	PNLIPRP3	pancreatic lipase-related protein 3	0.80
POF1B;1555383_a_at	POF1B	premature ovarian failure, 1B	1.52
POF1B;219756_s_at	POF1B	premature ovarian failure, 1B	1.24
PPL;203407_at	PPL	periplakin	1.08
PPP2R2C;223573_s_at	PPP2R2C	protein phosphatase 2 (formerly 2A), regula	1.30
PPP2R2C;223574_x_at	PPP2R2C	protein phosphatase 2 (formerly 2A), regula	1.19
PRSS8;202525_at	PRSS8	protease, serine, 8	1.09
PSAPL1;1564333_a_at	PSAPL1	prosaposin-like 1	1.46
PSORS1C2;220635_at	PSORS1C2	psoriasis susceptibility 1 candidate 2	1.74
PTGER3;210833_at	PTGER3	prostaglandin E receptor 3 (subtype EP3)	1.04
PTGER3;210834_s_at	PTGER3	prostaglandin E receptor 3 (subtype EP3)	1.22
PTGER3;213933_at	PTGER3	prostaglandin E receptor 3 (subtype EP3)	1.25
RAB25;218186_at	RAB25	RAB25, member RAS oncogene family	1.09
RAB38;219412_at	RAB38	RAB38, member RAS oncogene family	1.00
RDH12;242998_at	RDH12	retinol dehydrogenase 12 (all-trans/9-cis/11	1.10
RDH13;225467_s_at	RDH13	retinol dehydrogenase 13 (all-trans/9-cis)	1.13
RHBDL2;1552502_s_at	RHBDL2	rhomboid, veinlet-like 2 (Drosophila)	1.25
RHCG;219554_at	RHCG	Rh family, C glycoprotein	1.33
RHOD;209885_at	RHOD	ras homolog gene family, member D	1.15
RNASE7;233488_at	RNASE7	ribonuclease, RNase A family, 7	1.17
RNASE7;234699_at	RNASE7	ribonuclease, RNase A family, 7	1.18
RNASE7;234700_s_at	RNASE7	ribonuclease, RNase A family, 7	1.21
RNF39;219916_s_at	RNF39	ring finger protein 39	1.30
RORA;236266_at	RORA	RAR-related orphan receptor A	1.07
RPTN;1553454_at	RPTN	repetin	1.65
SBSN;235272_at	SBSN	suprabasin	1.19
SCEL;232056_at	SCEL	sciellin	1.02

SDCBP2;233565_s_at	SDCBP2	syndecan binding protein (syntenin) 2	1.01
SDR16C5;238017_at	SDR16C5	short chain dehydrogenase/reductase family	1.08
SDR9C7;1553077_at	SDR9C7	short chain dehydrogenase/reductase family	1.71
SERPINB12;1553057_at	SERPINB12	serpin peptidase inhibitor, clade B (ovalbum	1.41
SERPINB13;211361_s_at	SERPINB13	serpin peptidase inhibitor, clade B (ovalbum	1.45
SERPINB13;211362_s_at	SERPINB13	serpin peptidase inhibitor, clade B (ovalbum	1.47
SERPINB13;217272_s_at	SERPINB13	serpin peptidase inhibitor, clade B (ovalbum	1.41
SERPINB5;204855_at	SERPINB5	serpin peptidase inhibitor, clade B (ovalbum	1.02
SERPINB7;206421_s_at	SERPINB7	serpin peptidase inhibitor, clade B (ovalbum	1.54
SFN;209260_at	SFN	stratifin	1.02
SFN;33322_i_at	SFN	stratifin	0.98
SFN;33323_r_at	SFN	stratifin	0.94
SLC39A2;220413_at	SLC39A2	solute carrier family 39 (zinc transporter), m	1.93
SLC5A1;206628_at	SLC5A1	solute carrier family 5 (sodium/glucose cotra	1.59
SLC5A1;242773_at	SLC5A1	solute carrier family 5 (sodium/glucose cotra	1.74
SLURP1;214536_at	SLURP1	secreted LY6/PLAUR domain containing 1	1.51
SMPD3;219695_at	SMPD3	sphingomyelin phosphodiesterase 3, neutral	1.13
SPINK5;205185_at	SPINK5	serine peptidase inhibitor, Kazal type 5	1.13
SPINK7;223720_at	SPINK7	serine peptidase inhibitor, Kazal type 7 (puta	1.37
SPRR1A;213796_at	SPRR1A	small proline-rich protein 1A	1.22
SPRR1A;214549_x_at	SPRR1A	small proline-rich protein 1A	1.21
SPRR1B;205064_at	SPRR1B	small proline-rich protein 1B (cornifin)	1.14
SPRR2G;236119_s_at	SPRR2G	small proline-rich protein 2G	2.12
SPRR3;232082_x_at	SPRR3	small proline-rich protein 3	1.51
SPRR4;1552620_at	SPRR4	small proline-rich protein 4	0.63
SPTLC3;227752_at	SPTLC3	serine palmitoyltransferase, long chain base	1.43
SULT2B1;205759_s_at	SULT2B1	sulfotransferase family, cytosolic, 2B, memb	1.22
TGM1;206008_at	TGM1	transglutaminase 1 (K polypeptide epiderma	1.45
TGM3;206004_at	TGM3	transglutaminase 3 (E polypeptide, protein-g	1.22
TGM5;207911_s_at	TGM5	transglutaminase 5	0.92
TM7SF2;210130_s_at	TM7SF2	transmembrane 7 superfamily member 2	1.02
TMEM40;219503_s_at	TMEM40	transmembrane protein 40	1.07
TMEM40;222892_s_at	TMEM40	transmembrane protein 40	1.06
TMEM45A;219410_at	TMEM45A	transmembrane protein 45A	1.17
TMEM54;225536_at	TMEM54	transmembrane protein 54	1.02
TMEM79;223544_at	TMEM79	transmembrane protein 79	1.06
TMEM86A;227570_at	TMEM86A	transmembrane protein 86A	1.44
TMEM86A;242103_at	TMEM86A	transmembrane protein 86A	1.27
TMPRSS11E;220431_at	TMPRSS11E	transmembrane protease, serine 11E	0.46
TMPRSS13;223659_at	TMPRSS13	transmembrane protease, serine 13	1.39
TPRG1;229764_at	TPRG1	tumor protein p63 regulated 1	1.40
TREX2;211788_s_at	TREX2	three prime repair exonuclease 2	1.09
TRIM29;202504_at	TRIM29	tripartite motif-containing 29	0.94
TRIM29;211002_s_at	TRIM29	tripartite motif-containing 29	1.01
TRY6;215395_x_at	TRY6	trypsinogen C	1.04
TUFT1;205807_s_at	TUFT1	tuftelin 1	0.98
UPK1A;214624_at	UPK1A	uroplakin 1A	0.41
VSIG10L;238654_at	VSIG10L	V-set and immunoglobulin domain containir	1.28
WFDC12;1553081_at	WFDC12	WAP four-disulfide core domain 12	1.73
WFDC5;242204_at	WFDC5	WAP four-disulfide core domain 5	1.13

XKRX;230349_at	XKRX	XK, Kell blood group complex subunit-relate	1.37
ZNF750;219995_s_at	ZNF750	zinc finger protein 750	0.94
AHNAK2;212992_at	AHNAK2	AHNAK nucleoprotein 2	0.98
ARHGAP32;210791_s_at	ARHGAP32	Rho GTPase activating protein 32	1.12
ARHGAP32;242196_at	ARHGAP32	Rho GTPase activating protein 32	0.95
ARHGEF4;205109_s_at	ARHGEF4	Rho guanine nucleotide exchange factor (GE	0.97
ARHGEF5;204765_at	ARHGEF5	Rho guanine nucleotide exchange factor (GE	1.11
ATP13A4;1557136_at	ATP13A4	ATPase type 13A4	1.25
AZGP1;209309_at	AZGP1	alpha-2-glycoprotein 1, zinc-binding	1.03
AZGP1;217014_s_at	AZGP1	alpha-2-glycoprotein 1, zinc-binding	1.06
BAIAP2;209502_s_at	BAIAP2	BAI1-associated protein 2	0.99
BNIPL;236534_at	BNIPL	BCL2/adenovirus E1B 19kD interacting prote	1.07
BSPRY;218792_s_at	BSPRY	B-box and SPRY domain containing	1.27
C3orf57;238702_at	C3orf57	chromosome 3 open reading frame 57	1.10
C5orf46;1554195_a_at	C5orf46	chromosome 5 open reading frame 46	1.34
CCDC64B;235095_at	CCDC64B	coiled-coil domain containing 64B	1.00
CCDC85C;222809_x_at	CCDC85C	coiled-coil domain containing 85C	1.03
CELSR2;36499_at	CELSR2	cadherin, EGF LAG seven-pass G-type recept	1.03
CES8;228903_at	CES8	carboxylesterase 8 (putative)	1.09
CXCL14;237038_at	CXCL14	chemokine (C-X-C motif) ligand 14	0.95
D4S234E;209570_s_at	D4S234E	DNA segment on chromosome 4 (unique) 23	1.06
DENND2C;230769_at	DENND2C	DENN/MADD domain containing 2C	1.11
DNAJB2;202500_at	DNAJB2	DnaJ (Hsp40) homolog, subfamily B, membe	1.13
DSC3;206032_at	DSC3	desmocollin 3	0.92
DUOX1;219597_s_at	DUOX1	dual oxidase 1	1.06
DUOXA1;1555404_a_at	DUOXA1	dual oxidase maturation factor 1	1.07
EFNA3;210132_at	EFNA3	ephrin-A3	1.05
EMILIN3;228307_at	EMILIN3	elastin microfibril interfacer 3	0.92
ENDOU;206605_at	ENDOU	endonuclease, polyU-specific	0.87
EPN2;203464_s_at	EPN2	epsin 2	1.00
FAM160A1;242687_at	FAM160A1	family with sequence similarity 160, membe	1.16
FAM83H;226129_at	FAM83H	family with sequence similarity 83, member	0.95
FAM84A;234331_s_at	FAM84A	family with sequence similarity 84, member	0.75
FGF11;227271_at	FGF11	fibroblast growth factor 11	1.05
GAN;220124_at	GAN	gigaxonin	1.40
GGT6;236225_at	GGT6	gamma-glutamyltransferase 6	0.96
GJB5;206156_at	GJB5	gap junction protein, beta 5, 31.1kDa	1.23
GPR115;237690_at	GPR115	G protein-coupled receptor 115	1.09
GRAMD1C;219313_at	GRAMD1C	GRAM domain containing 1C	0.95
HNRNPC;235500_at	HNRNPC	heterogeneous nuclear ribonucleoprotein C	1.02
IDE;203327_at	IDE	insulin-degrading enzyme	1.38
IL1F7;221470_s_at	IL1F7	interleukin 1 family, member 7 (zeta)	1.64
IL1F7;224555_x_at	IL1F7	interleukin 1 family, member 7 (zeta)	1.63
IL20RB;228575_at	IL20RB	interleukin 20 receptor beta	1.00
IL22RA1;220056_at	IL22RA1	interleukin 22 receptor, alpha 1	1.46
IRX2;228462_at	IRX2	iroquois homeobox 2	0.85
KCNK7;220412_x_at	KCNK7	potassium channel, subfamily K, member 7	1.00
KCNK7;224008_s_at	KCNK7	potassium channel, subfamily K, member 7	0.94
KCNK7;224055_x_at	KCNK7	potassium channel, subfamily K, member 7	0.96
KIAA1543;1568617_a_at	KIAA1543	KIAA1543	0.84

KLF5;209211_at	KLF5	Kruppel-like factor 5 (intestinal)	0.93
KLF8;219930_at	KLF8	Kruppel-like factor 8	0.88
LNX1;223611_s_at	LNX1	ligand of numb-protein X 1	1.09
LOC100288860;239127_a	LOC100288860	hypothetical protein LOC100288860	1.04
MPZL3;227747_at	MPZL3	myelin protein zero-like 3	1.34
MYO6;203215_s_at	MYO6	myosin VI	1.09
NA;1562921_at	NA	NA	0.83
NA;1568932_at	NA	NA	0.95
NA;202712_s_at	NA	NA	0.85
NA;230778_at	NA	NA	1.09
NA;231311_at	NA	NA	1.01
NA;232202_at	NA	NA	0.98
NA;232699_at	NA	NA	1.17
NA;235651_at	NA	NA	1.03
NA;240361_at	NA	NA	1.19
NA;241300_at	NA	NA	1.40
NA;241356_at	NA	NA	1.05
NA;241890_at	NA	NA	1.27
NA;244107_at	NA	NA	0.93
NDFIP2;224801_at	NDFIP2	Nedd4 family interacting protein 2	0.88
NEBL;203962_s_at	NEBL	nebulette	0.97
NIPAL2;227001_at	NIPAL2	NIPA-like domain containing 2	1.02
OSBPL6;223805_at	OSBPL6	oxysterol binding protein-like 6	1.12
PDZD2;209493_at	PDZD2	PDZ domain containing 2	0.93
PERP;236009_at	PERP	PERP, TP53 apoptosis effector	1.10
PIGN;232101_s_at	PIGN	phosphatidylinositol glycan anchor biosynth	1.00
PITPNM3;230076_at	PITPNM3	PITPNM family member 3	0.93
PLA2G3;220780_at	PLA2G3	phospholipase A2, group III	1.42
PLAC2;229385_s_at	PLAC2	placenta-specific 2 (non-protein coding)	1.06
PPP1R13L;218849_s_at	PPP1R13L	protein phosphatase 1, regulatory (inhibitor	0.99
PPP1R14C;226907_at	PPP1R14C	protein phosphatase 1, regulatory (inhibitor	1.11
PPP2R2C;228010_at	PPP2R2C	protein phosphatase 2 (formerly 2A), regula	0.94
PTGER3;210375_at	PTGER3	prostaglandin E receptor 3 (subtype EP3)	1.11
PTK6;1553114_a_at	PTK6	PTK6 protein tyrosine kinase 6	1.19
RAB40C;227698_s_at	RAB40C	RAB40C, member RAS oncogene family	0.93
RAET1E;1552777_a_at	RAET1E	retinoic acid early transcript 1E	1.30
RAPGEFL1;218657_at	RAPGEFL1	Rap guanine nucleotide exchange factor (GE	0.99
RASSF9;210335_at	RASSF9	Ras association (RalGDS/AF-6) domain famil	0.87
RDH13;1559190_s_at	RDH13	retinol dehydrogenase 13 (all-trans/9-cis)	1.03
RHOV;241990_at	RHOV	ras homolog gene family, member V	1.28
SCEL;206884_s_at	SCEL	sciellin	1.05
SDR42E1;229522_at	SDR42E1	short chain dehydrogenase/reductase famil	1.13
SERPINA12;1552544_at	SERPINA12	serpin peptidase inhibitor, clade A (alpha-1 a	1.33
STARD5;213820_s_at	STARD5	StAR-related lipid transfer (START) domain c	1.16
SYT8;232802_at	SYT8	synaptotagmin VIII	0.96
TOB2;222243_s_at	TOB2	transducer of ERBB2, 2	1.01
TP63;209863_s_at	TP63	tumor protein p63	0.89
UNQ1887;224639_at	UNQ1887	signal peptide peptidase 3	1.04
WWC1;213085_s_at	WWC1	WW and C2 domain containing 1	1.04
XG;1554062_at	XG	Xg blood group	1.25

ZBTB7C;227782_at	ZBTB7C	zinc finger and BTB domain containing 7C	1.09
ZNF57;1554628_at	ZNF57	zinc finger protein 57	0.99
ZNF770;220608_s_at	ZNF770	zinc finger protein 770	0.86
ADH7;210505_at	ADH7	alcohol dehydrogenase 7 (class IV), mu or sig	1.00
AGR2;209173_at	AGR2	anterior gradient homolog 2 (Xenopus laevis	0.47
AGR2;228969_at	AGR2	anterior gradient homolog 2 (Xenopus laevis	0.60
ALDH3A1;205623_at	ALDH3A1	aldehyde dehydrogenase 3 family, memberA	0.93
ATP12A;207367_at	ATP12A	ATPase, H+/K+ transporting, nongastric, alph	0.57
C10orf81;1554190_s_at	C10orf81	chromosome 10 open reading frame 81	1.32
C10orf81;219857_at	C10orf81	chromosome 10 open reading frame 81	1.50
C11orf88;1568606_at	C11orf88	chromosome 11 open reading frame 88	1.10
C13orf30;1556711_at	C13orf30	chromosome 13 open reading frame 30	1.06
C1orf192;231077_at	C1orf192	chromosome 1 open reading frame 192	1.27
C1orf88;228100_at	C1orf88	chromosome 1 open reading frame 88	0.92
C20orf114;226067_at	C20orf114	chromosome 20 open reading frame 114	1.14
C20orf85;229542_at	C20orf85	chromosome 20 open reading frame 85	1.15
C7orf57;1557636_a_at	C7orf57	chromosome 7 open reading frame 57	1.05
C9orf24;229012_at	C9orf24	chromosome 9 open reading frame 24	1.15
CAPSL;236085_at	CAPSL	calcyphosine-like	1.03
CCDC17;236320_at	CCDC17	coiled-coil domain containing 17	0.87
CHST9;223737_x_at	CHST9	carbohydrate (N-acetylgalactosamine 4-0) su	1.00
CHST9;224400_s_at	CHST9	carbohydrate (N-acetylgalactosamine 4-0) su	0.96
CXCL17;226960_at	CXCL17	chemokine (C-X-C motif) ligand 17	1.16
CYP2B7P1;210272_at	CYP2B7P1	cytochrome P450, family 2, subfamily B, poly	0.75
CYP2F1;207913_at	CYP2F1	cytochrome P450, family 2, subfamily F, poly	1.09
CYP4X1;227702_at	CYP4X1	cytochrome P450, family 4, subfamily X, poly	1.05
DNAI1;220125_at	DNAI1	dynein, axonemal, intermediate chain 1	1.21
DYDC2;239733_at	DYDC2	DPY30 domain containing 2	1.04
EFCAB1;220156_at	EFCAB1	EF-hand calcium binding domain 1	1.12
ELF3;201510_at	ELF3	E74-like factor 3 (ets domain transcription fa	1.49
ELF3;210827_s_at	ELF3	E74-like factor 3 (ets domain transcription fa	1.19
ELF3;229842_at	ELF3	E74-like factor 3 (ets domain transcription fa	1.48
FGFR3;204380_s_at	FGFR3	fibroblast growth factor receptor 3	0.87
FOXA1;204667_at	FOXA1	forkhead box A1	1.07
FOXJ1;205906_at	FOXJ1	forkhead box J1	1.11
FUT2;210608_s_at	FUT2	fucosyltransferase 2 (secretor status include	1.22
FUT6;210398_x_at	FUT6	fucosyltransferase 6 (alpha (1,3) fucosyltrans	1.05
FUT6;210399_x_at	FUT6	fucosyltransferase 6 (alpha (1,3) fucosyltrans	1.24
FUT6;211465_x_at	FUT6	fucosyltransferase 6 (alpha (1,3) fucosyltrans	1.15
FUT6;211885_x_at	FUT6	fucosyltransferase 6 (alpha (1,3) fucosyltrans	1.18
GPR110;235988_at	GPR110	G protein-coupled receptor 110	1.07
GPR110;238689_at	GPR110	G protein-coupled receptor 110	1.19
LRRC10B;236666_s_at	LRRC10B	leucine rich repeat containing 10B	0.86
LRRC23;206076_at	LRRC23	leucine rich repeat containing 23	0.95
LRRC46;230601_s_at	LRRC46	leucine rich repeat containing 46	1.00
MS4A8B;224355_s_at	MS4A8B	membrane-spanning 4-domains, subfamily A	1.04
MUC1;207847_s_at	MUC1	mucin 1, cell surface associated	0.30
MUC1;211695_x_at	MUC1	mucin 1, cell surface associated	0.52
MUC1;213693_s_at	MUC1	mucin 1, cell surface associated	0.41
MUC20;226622_at	MUC20	mucin 20, cell surface associated	0.63

MUC4;217110_s_at	MUC4	mucin 4, cell surface associated	1.08
NA;1561368_at	NA	NA	1.05
NA;206754_s_at	NA	NA	0.78
NA;222271_at	NA	NA	1.10
NA;235892_at	NA	NA	1.13
NA;236489_at	NA	NA	1.11
OMG;238720_at	OMG	oligodendrocyte myelin glycoprotein	1.02
PIGR;204213_at	PIGR	polymeric immunoglobulin receptor	1.14
PIGR;226147_s_at	PIGR	polymeric immunoglobulin receptor	1.39
PLUNC;220542_s_at	PLUNC	palate, lung and nasal epithelium associated	1.05
POU2AF1;1569675_at	POU2AF1	POU class 2 associating factor 1	0.94
PRR15L;219127_at	PRR15L	proline rich 15-like	1.54
PSCA;205319_at	PSCA	prostate stem cell antigen	1.17
RSPH1;230093_at	RSPH1	radial spoke head 1 homolog (Chlamydomor	1.09
SCGB3A1;230378_at	SCGB3A1	secretoglobin, family 3A, member 1	1.72
SERPINB11;1552463_at	SERPINB11	serpin peptidase inhibitor, clade B (ovalbum	0.91
SLC34A2;204124_at	SLC34A2	solute carrier family 34 (sodium phosphate),	1.17
SLC44A4;1555203_s_at	SLC44A4	solute carrier family 44, member 4	1.12
SLC44A4;205597_at	SLC44A4	solute carrier family 44, member 4	0.89
SNTN;239150_at	SNTN	sentan, cilia apical structure protein	1.07
SPAG6;210033_s_at	SPAG6	sperm associated antigen 6	1.21
SPEF1;216119_s_at	SPEF1	sperm flagellar 1	1.23
ST6GALNAC1;227725_at	ST6GALNAC1	ST6 (alpha-N-acetyl-neuraminyl-2,3-beta-gal	0.98
STATH;206835_at	STATH	statherin	0.97
TMC4;226403_at	TMC4	transmembrane channel-like 4	1.11
TMEM190;1552594_at	TMEM190	transmembrane protein 190	1.19
TMPRSS4;218960_at	TMPRSS4	transmembrane protease, serine 4	1.21
TSPAN1;209114_at	TSPAN1	tetraspanin 1	1.18
VSIG2;228232_s_at	VSIG2	V-set and immunoglobulin domain containir	1.24
VSTM2L;226973_at	VSTM2L	V-set and transmembrane domain containin	1.01
WDR16;239916_at	WDR16	WD repeat domain 16	1.05
WFDC2;203892_at	WFDC2	WAP four-disulfide core domain 2	1.25
ZMYND10;205714_s_at	ZMYND10	zinc finger, MYND-type containing 10	1.01
ZMYND10;216663_s_at	ZMYND10	zinc finger, MYND-type containing 10	1.17
HLA-A;213932_x_at	HLA-A	major histocompatibility complex, class I, A	0.99
HLA-A;215313_x_at	HLA-A	major histocompatibility complex, class I, A	1.04
HLA-B;208729_x_at	HLA-B	major histocompatibility complex, class I, B	1.07
HLA-B;209140_x_at	HLA-B	major histocompatibility complex, class I, B	1.05
HLA-B;211911_x_at	HLA-B	major histocompatibility complex, class I, B	1.10
HLA-C;208812_x_at	HLA-C	major histocompatibility complex, class I, C	0.95
HLA-C;211799_x_at	HLA-C	major histocompatibility complex, class I, C	1.02
HLA-C;214459_x_at	HLA-C	major histocompatibility complex, class I, C	0.99
HLA-C;216526_x_at	HLA-C	major histocompatibility complex, class I, C	1.01
HLA-E;200905_x_at	HLA-E	major histocompatibility complex, class I, E	0.94
HLA-E;217456_x_at	HLA-E	major histocompatibility complex, class I, E	0.95
HLA-F;204806_x_at	HLA-F	major histocompatibility complex, class I, F	0.94
HLA-F;221875_x_at	HLA-F	major histocompatibility complex, class I, F	0.91
HLA-G;210514_x_at	HLA-G	major histocompatibility complex, class I, G	1.02
HLA-G;211528_x_at	HLA-G	major histocompatibility complex, class I, G	0.98
HLA-G;211529_x_at	HLA-G	major histocompatibility complex, class I, G	1.01

HLA-G;211530_x_at	HLA-G	major histocompatibility complex, class I, G	1.05
HLA-J;217436_x_at	HLA-J	major histocompatibility complex, class I, J (	1.12
ACADL;206068_s_at	ACADL	acyl-Coenzyme A dehydrogenase, long chain	1.09
ACADL;206069_s_at	ACADL	acyl-Coenzyme A dehydrogenase, long chain	0.96
ANO1;218804_at	ANO1	anoctamin 1, calcium activated chloride cha	0.85
C11orf52;238805_at	C11orf52	chromosome 11 open reading frame 52	0.98
CNGA1;206417_at	CNGA1	cyclic nucleotide gated channel alpha 1	1.34
CYP39A1;1553977_a_at	CYP39A1	cytochrome P450, family 39, subfamily A, pc	1.14
CYP39A1;220432_s_at	CYP39A1	cytochrome P450, family 39, subfamily A, pc	0.97
EPHX2;209368_at	EPHX2	epoxide hydrolase 2, cytoplasmic	0.97
HYAL1;210619_s_at	HYAL1	hyaluronoglucosaminidase 1	1.40
NA;1556122_at	NA	NA	1.08
NA;214415_at	NA	NA	0.80
NA;231704_at	NA	NA	0.83
NA;235937_at	NA	NA	1.16
SEC16B;1552880_at	SEC16B	SEC16 homolog B (S. cerevisiae)	0.78
TRPM8;243483_at	TRPM8	transient receptor potential cation channel,	0.93
UNC5CL;231008_at	UNC5CL	unc-5 homolog C (C. elegans)-like	0.93
BEGAIN;220795_s_at	BEGAIN	brain-enriched guanylate kinase-associated I	1.11
CHRM3;214596_at	CHRM3	cholinergic receptor, muscarinic 3	1.17
EML5;1568777_at	EML5	echinoderm microtubule associated protein	0.87
NA;231214_at	NA	NA	0.96
NA;235079_at	NA	NA	0.79
NA;239708_at	NA	NA	1.78
NA;241873_at	NA	NA	1.09
NA;243339_at	NA	NA	1.09
NA;244114_x_at	NA	NA	0.76
NA;244359_s_at	NA	NA	0.74
NA;244532_x_at	NA	NA	0.78
NBLA00301;236141_at	NBLA00301	Nbla00301	1.82
PCLO;210650_s_at	PCLO	piccolo (presynaptic cytomatrix protein)	0.88
RIMBP2;214811_at	RIMBP2	RIMS binding protein 2	0.75
TFAP2B;1553394_a_at	TFAP2B	transcription factor AP-2 beta (activating enl	0.79
TFAP2B;214451_at	TFAP2B	transcription factor AP-2 beta (activating enl	0.88
CD74;209619_at	CD74	CD74 molecule, major histocompatibility cor	0.95
HLA-DMB;203932_at	HLA-DMB	major histocompatibility complex, class II, D	0.94
HLA-DPA1;211990_at	HLA-DPA1	major histocompatibility complex, class II, D	0.98
HLA-DPA1;211991_s_at	HLA-DPA1	major histocompatibility complex, class II, D	0.93
HLA-DPA1;213537_at	HLA-DPA1	major histocompatibility complex, class II, D	1.06
HLA-DPB1;201137_s_at	HLA-DPB1	major histocompatibility complex, class II, D	0.72
HLA-DRA;208894_at	HLA-DRA	major histocompatibility complex, class II, D	0.92
HLA-DRA;210982_s_at	HLA-DRA	major histocompatibility complex, class II, D	0.98
HLA-DRB4;208306_x_at	HLA-DRB4	major histocompatibility complex, class II, D	0.96
HLA-DRB6;217362_x_at	HLA-DRB6	major histocompatibility complex, class II, D	0.93
NA;204670_x_at	NA	NA	1.24
NA;209312_x_at	NA	NA	1.03
NA;212671_s_at	NA	NA	0.95
NA;215193_x_at	NA	NA	0.95
NA;217478_s_at	NA	NA	1.00
ITGB4;204989_s_at	ITGB4	integrin, beta 4	0.98

ITGB4;204990_s_at	ITGB4	integrin, beta 4	1.07
ITGB4;211905_s_at	ITGB4	integrin, beta 4	0.91
LAMA3;203726_s_at	LAMA3	laminin, alpha 3	0.97
LAMB3;209270_at	LAMB3	laminin, beta 3	1.07
LAMC2;202267_at	LAMC2	laminin, gamma 2	0.91
LAMC2;207517_at	LAMC2	laminin, gamma 2	0.92
NA;1556773_at	NA	NA	0.84
PADI3;220779_at	PADI3	peptidyl arginine deiminase, type III	0.65
PTHLH;206300_s_at	PTHLH	parathyroid hormone-like hormone	0.95
PTHLH;210355_at	PTHLH	parathyroid hormone-like hormone	0.66
PTHLH;211756_at	PTHLH	parathyroid hormone-like hormone	0.62
TP63;211194_s_at	TP63	tumor protein p63	0.87
TP63;211834_s_at	TP63	tumor protein p63	1.13
WDR66;1555007_s_at	WDR66	WD repeat domain 66	0.89
C19orf33;223631_s_at	C19orf33	chromosome 19 open reading frame 33	1.23
FGFBP1;205014_at	FGFBP1	fibroblast growth factor binding protein 1	1.58
FXYD3;202489_s_at	FXYD3	FXYD domain containing ion transport regula	1.07
KRT5;201820_at	KRT5	keratin 5	0.99
PERP;217744_s_at	PERP	PERP, TP53 apoptosis effector	0.96
PERP;222392_x_at	PERP	PERP, TP53 apoptosis effector	1.03
PTK6;206482_at	PTK6	PTK6 protein tyrosine kinase 6	1.02
RHBDL2;1554895_a_at	RHBDL2	rhomboid, veinlet-like 2 (Drosophila)	1.05
RHBDL2;1554897_s_at	RHBDL2	rhomboid, veinlet-like 2 (Drosophila)	1.21
S100A14;218677_at	S100A14	S100 calcium binding protein A14	0.94
S100A2;204268_at	S100A2	S100 calcium binding protein A2	0.92
SDC1;201287_s_at	SDC1	syndecan 1	0.96
TMEM184A;1558281_a_a	TMEM184A	transmembrane protein 184A	1.07
TRIM7;223694_at	TRIM7	tripartite motif-containing 7	1.15
COL12A1;225664_at	COL12A1	collagen, type XII, alpha 1	0.95
COL1A1;1556499_s_at	COL1A1	collagen, type I, alpha 1	0.86
COL1A1;202310_s_at	COL1A1	collagen, type I, alpha 1	0.90
COL1A2;202403_s_at	COL1A2	collagen, type I, alpha 2	0.94
COL1A2;202404_s_at	COL1A2	collagen, type I, alpha 2	0.83
COL3A1;201852_x_at	COL3A1	collagen, type III, alpha 1	0.83
COL3A1;211161_s_at	COL3A1	collagen, type III, alpha 1	0.87
COL3A1;215076_s_at	COL3A1	collagen, type III, alpha 1	0.83
COL6A1;213428_s_at	COL6A1	collagen, type VI, alpha 1	1.02
COL6A2;209156_s_at	COL6A2	collagen, type VI, alpha 2	1.16
COL6A3;201438_at	COL6A3	collagen, type VI, alpha 3	0.90
MXRA8;213422_s_at	MXRA8	matrix-remodelling associated 8	1.12
ACVR1C;1552519_at	ACVR1C	activin A receptor, type IC	0.42
ADIPOQ;207175_at	ADIPOQ	adiponectin, C1Q and collagen domain conta	0.68
AOC3;204894_s_at	AOC3	amine oxidase, copper containing 3 (vascula	0.84
AQP7;206955_at	AQP7	aquaporin 7	0.71
C14orf180;1558421_a_at	C14orf180	chromosome 14 open reading frame 180	1.19
CIDEC;219398_at	CIDEC	cell death-inducing DFFA-like effector c	0.80
KCNIP2;223727_at	KCNIP2	Kv channel interacting protein 2	0.86
LIPE;213855_s_at	LIPE	lipase, hormone-sensitive	0.79
MRAP;1554044_a_at	MRAP	melanocortin 2 receptor accessory protein	0.86
MRAP;1555740_a_at	MRAP	melanocortin 2 receptor accessory protein	0.68

PLIN1;205913_at	PLIN1	perilipin 1	0.82
PLIN4;228409_at	PLIN4	perilipin 4	0.96
ACVRL1;226950_at	ACVRL1	activin A receptor type II-like 1	1.31
ECSCR;227779_at	ECSCR	endothelial cell-specific chemotaxis regulato	0.96
ECSCR;228339_at	ECSCR	endothelial cell-specific chemotaxis regulato	0.95
ESAM;225369_at	ESAM	endothelial cell adhesion molecule	0.93
MMRN2;219091_s_at	MMRN2	multimerin 2	0.93
MMRN2;236262_at	MMRN2	multimerin 2	0.88

Human_cell-cluster	MCL_2.2_6
Kerantincytes	Cluster0003
Kerantincytes	Cluster0003
Kerantincytes	Cluster0003
Kerantincytes	Cluster0003
Kerantincytes	Cluster0003
Kerantincytes	Cluster0003
Kerantincytes	Cluster0003
Kerantincytes	Cluster0003
Kerantincytes	Cluster0003
Kerantincytes	Cluster0003
Kerantincytes	Cluster0003
Kerantincytes	Cluster0003
Kerantincytes	Cluster0003
Kerantincytes	Cluster0003
Kerantincytes	Cluster0003
Kerantincytes	Cluster0003
Kerantincytes	Cluster0003
Kerantincytes	Cluster0003
Kerantincytes	Cluster0003
Kerantincytes	Cluster0003
Kerantincytes	Cluster0003
Kerantincytes	Cluster0003
Kerantincytes	Cluster0003
Kerantincytes	Cluster0003
Kerantincytes	Cluster0003
Kerantincytes	Cluster0003
Kerantincytes	Cluster0003
Kerantincytes	Cluster0003
Kerantincytes	Cluster0003
Kerantincytes	Cluster0003
Kerantincytes	Cluster0003
Kerantincytes	Cluster0003
Kerantincytes	Cluster0003
Kerantincytes	Cluster0003
Kerantincytes	Cluster0003
Kerantincytes	Cluster0003
Kerantincytes	Cluster0003
Kerantincytes	Cluster0003
Kerantincytes	Cluster0003
Kerantincytes	Cluster0003
Kerantincytes	Cluster0003
Kerantincytes	Cluster0003
Kerantincytes	Cluster0003
Kerantincytes	Cluster0003
Kerantincytes	Cluster0003
Kerantincytes	Cluster0003
Kerantincytes	Cluster0003
Kerantincytes	Cluster0003
Kerantincytes	Cluster0003

Kerantincytes	Cluster0003
Kerantincytes	Cluster0003
Kerantincytes	Cluster0003
Kerantincytes	Cluster0003
Kerantincytes	Cluster0003
Kerantincytes	Cluster0003
Kerantincytes	Cluster0003
Kerantincytes	Cluster0003
Kerantincytes	Cluster0003
Kerantincytes	Cluster0003
Kerantincytes	Cluster0003
Kerantincytes	Cluster0003
Kerantincytes	Cluster0003
Kerantincytes	Cluster0003
Kerantincytes	Cluster0003
Kerantincytes	Cluster0003
Kerantincytes	Cluster0003
Kerantincytes	Cluster0003
Kerantincytes	Cluster0003
Kerantincytes	Cluster0003
Kerantincytes	Cluster0003
Kerantincytes	Cluster0003
Kerantincytes	Cluster0003
Kerantincytes	Cluster0003
Kerantincytes	Cluster0003
Kerantincytes	Cluster0003
Kerantincytes	Cluster0003
Kerantincytes	Cluster0003
Kerantincytes	Cluster0003
Kerantincytes	Cluster0003
Kerantincytes	Cluster0003
Kerantincytes	Cluster0003
Kerantincytes	Cluster0003
Kerantincytes	Cluster0003
Kerantincytes	Cluster0003
Kerantincytes	Cluster0003
Kerantincytes	Cluster0003
Kerantincytes	Cluster0003
Kerantincytes	Cluster0003
Kerantincytes	Cluster0003
Kerantincytes	Cluster0003
Kerantincytes	Cluster0003
Kerantincytes	Cluster0003
Kerantincytes	Cluster0003
Kerantincytes	Cluster0003
Kerantincytes	Cluster0003
Kerantincytes	Cluster0003
Kerantincytes	Cluster0003
Kerantincytes	Cluster0003
Kerantincytes	Cluster0003

Kerantincytes	Cluster0003
Kerantincytes	Cluster0003
Kerantincytes	Cluster0003
Kerantincytes	Cluster0003
Kerantincytes	Cluster0003
Kerantincytes	Cluster0003
Kerantincytes	Cluster0003
Kerantincytes	Cluster0003
Kerantincytes	Cluster0003
Kerantincytes	Cluster0003
Kerantincytes	Cluster0003
Kerantincytes	Cluster0003
Kerantincytes	Cluster0003
Kerantincytes	Cluster0003
Kerantincytes	Cluster0003
Kerantincytes	Cluster0003
Kerantincytes	Cluster0003
Kerantincytes	Cluster0003
Kerantincytes	Cluster0003
Kerantincytes	Cluster0003
Kerantincytes	Cluster0003
Kerantincytes	Cluster0003
Kerantincytes	Cluster0003
Kerantincytes	Cluster0003
Kerantincytes	Cluster0003
Kerantincytes	Cluster0003
Kerantincytes	Cluster0003
Kerantincytes	Cluster0003
Kerantincytes	Cluster0003
Kerantincytes	Cluster0003
Kerantincytes	Cluster0003
Kerantincytes	Cluster0003
Kerantincytes	Cluster0003
Kerantincytes	Cluster0003
Kerantincytes	Cluster0003
Kerantincytes	Cluster0003
Kerantincytes	Cluster0003
Kerantincytes	Cluster0003
Kerantincytes	Cluster0003
Kerantincytes	Cluster0003
Kerantincytes	Cluster0003
Kerantincytes	Cluster0003
Kerantincytes	Cluster0003
Kerantincytes	Cluster0003
Kerantincytes	Cluster0003
Kerantincytes	Cluster0003
Kerantincytes	Cluster0003
Kerantincytes	Cluster0003
Kerantincytes	Cluster0003
Kerantincytes	Cluster0003

Kerantincytes	Cluster0003
Kerantincytes	Cluster0003
Kerantincytes	Cluster0003
Kerantincytes	Cluster0003
Kerantincytes	Cluster0003
Kerantincytes	Cluster0003
Kerantincytes	Cluster0003
Kerantincytes	Cluster0003
Kerantincytes	Cluster0003
Kerantincytes	Cluster0003
Kerantincytes	Cluster0003
Kerantincytes	Cluster0003
Kerantincytes	Cluster0003
Kerantincytes	Cluster0003
Kerantincytes	Cluster0003
Kerantincytes	Cluster0003
Kerantincytes	Cluster0003
Kerantincytes	Cluster0003
Kerantincytes	Cluster0003
Kerantincytes	Cluster0003
Kerantincytes	Cluster0003
Kerantincytes	Cluster0003
Kerantincytes	Cluster0003
Kerantincytes	Cluster0003
Kerantincytes	Cluster0003
Kerantincytes	Cluster0003
Kerantincytes	Cluster0003
Kerantincytes	Cluster0003
Kerantincytes	Cluster0003
Kerantincytes	Cluster0003
Kerantincytes	Cluster0003
Kerantincytes	Cluster0003
Kerantincytes	Cluster0003
Kerantincytes	Cluster0003
Kerantincytes	Cluster0003
Kerantincytes	Cluster0003
Kerantincytes	Cluster0003
Kerantincytes	Cluster0003
Kerantincytes	Cluster0003
Kerantincytes	Cluster0003
Kerantincytes	Cluster0003
Kerantincytes	Cluster0003
Kerantincytes	Cluster0003
Kerantincytes	Cluster0003
Kerantincytes	Cluster0003
Kerantincytes	Cluster0003
Kerantincytes	Cluster0003
Kerantincytes	Cluster0003
Kerantincytes	Cluster0003
Kerantincytes	Cluster0003

Kerantincytes	Cluster0003
Kerantincytes	Cluster0003
Kerantincytes	Cluster0003
Kerantincytes	Cluster0003
Kerantincytes	Cluster0003
Kerantincytes	Cluster0003
Kerantincytes	Cluster0003
Kerantincytes	Cluster0003
Kerantincytes	Cluster0003
Kerantincytes	Cluster0003
Kerantincytes	Cluster0003
Kerantincytes	Cluster0003
Kerantincytes	Cluster0003
Kerantincytes	Cluster0003
Kerantincytes	Cluster0003
Kerantincytes	Cluster0003
Kerantincytes	Cluster0003
Kerantincytes	Cluster0003
Kerantincytes	Cluster0003
Kerantincytes	Cluster0003
Kerantincytes	Cluster0003
Kerantincytes	Cluster0003
Kerantincytes	Cluster0003
Kerantincytes	Cluster0003
Kerantincytes	Cluster0003
Kerantincytes	Cluster0003
Kerantincytes	Cluster0003
Kerantincytes	Cluster0003
Kerantincytes	Cluster0003
Kerantincytes	Cluster0003
Kerantincytes	Cluster0003
Kerantincytes	Cluster0003
Kerantincytes	Cluster0003
Kerantincytes	Cluster0003
Kerantincytes	Cluster0003
Kerantincytes	Cluster0003
Kerantincytes	Cluster0003
Kerantincytes	Cluster0003
Kerantincytes	Cluster0003
Kerantincytes	Cluster0003
Kerantincytes	Cluster0003
Kerantincytes	Cluster0003
Kerantincytes	Cluster0003
Kerantincytes	Cluster0003
Kerantincytes	Cluster0003
Kerantincytes	Cluster0003
Kerantincytes	Cluster0003
Kerantincytes	Cluster0003
Kerantincytes	Cluster0003
Kerantincytes	Cluster0003

Kerantincytes	Cluster0003
Kerantincytes	Cluster0003
Kerantincytes	Cluster0003
Kerantincytes	Cluster0003
Kerantincytes	Cluster0003
Kerantincytes	Cluster0003
Kerantincytes	Cluster0003
Kerantincytes	Cluster0003
Kerantincytes	Cluster0003
Kerantincytes	Cluster0003
Kerantincytes	Cluster0003
Kerantincytes	Cluster0003
Kerantincytes	Cluster0003
Kerantincytes	Cluster0003
Kerantincytes	Cluster0003
Kerantincytes	Cluster0003
Kerantincytes	Cluster0003
Kerantincytes	Cluster0003
Kerantincytes	Cluster0003
Kerantincytes	Cluster0003
Kerantincytes	Cluster0003
Kerantincytes	Cluster0003
Kerantincytes	Cluster0003
Kerantincytes	Cluster0003
Kerantincytes	Cluster0003
Kerantincytes	Cluster0003
Kerantincytes	Cluster0003
Kerantincytes	Cluster0003
Kerantincytes	Cluster0003
Kerantincytes	Cluster0003
Kerantincytes	Cluster0003
Kerantincytes	Cluster0003
Kerantincytes	Cluster0003
Kerantincytes	Cluster0003
Kerantincytes	Cluster0003
Kerantincytes	Cluster0003
Kerantincytes	Cluster0003
Kerantincytes	Cluster0003
Kerantincytes	Cluster0003
Kerantincytes	Cluster0003
Kerantincytes	Cluster0003
Kerantincytes	Cluster0003
Kerantincytes	Cluster0003
Kerantincytes	Cluster0003
Kerantincytes	Cluster0003
Kerantincytes	Cluster0003
Kerantincytes	Cluster0003
Kerantincytes	Cluster0003
Kerantincytes	Cluster0003
Kerantincytes	Cluster0003

Kerantincytes	Cluster0003
Kerantincytes	Cluster0003
Kerantincytes	Cluster0008
Kerantincytes	Cluster0008
Kerantincytes	Cluster0008
Kerantincytes	Cluster0008
Kerantincytes	Cluster0008
Kerantincytes	Cluster0008
Kerantincytes	Cluster0008
Kerantincytes	Cluster0008
Kerantincytes	Cluster0008
Kerantincytes	Cluster0008
Kerantincytes	Cluster0008
Kerantincytes	Cluster0008
Kerantincytes	Cluster0008
Kerantincytes	Cluster0008
Kerantincytes	Cluster0008
Kerantincytes	Cluster0008
Kerantincytes	Cluster0008
Kerantincytes	Cluster0008
Kerantincytes	Cluster0008
Kerantincytes	Cluster0008
Kerantincytes	Cluster0008
Kerantincytes	Cluster0008
Kerantincytes	Cluster0008
Kerantincytes	Cluster0008
Kerantincytes	Cluster0008
Kerantincytes	Cluster0008
Kerantincytes	Cluster0008
Kerantincytes	Cluster0008
Kerantincytes	Cluster0008
Kerantincytes	Cluster0008
Kerantincytes	Cluster0008
Kerantincytes	Cluster0008
Kerantincytes	Cluster0008
Kerantincytes	Cluster0008
Kerantincytes	Cluster0008
Kerantincytes	Cluster0008
Kerantincytes	Cluster0008
Kerantincytes	Cluster0008
Kerantincytes	Cluster0008
Kerantincytes	Cluster0008
Kerantincytes	Cluster0008
Kerantincytes	Cluster0008
Kerantincytes	Cluster0008
Kerantincytes	Cluster0008
Kerantincytes	Cluster0008
Kerantincytes	Cluster0008
Kerantincytes	Cluster0008
Kerantincytes	Cluster0008

Kerantincytes	Cluster0008
Kerantincytes	Cluster0008
Kerantincytes	Cluster0008
Kerantincytes	Cluster0008
Kerantincytes	Cluster0008
Kerantincytes	Cluster0008
Kerantincytes	Cluster0008
Kerantincytes	Cluster0008
Kerantincytes	Cluster0008
Kerantincytes	Cluster0008
Kerantincytes	Cluster0008
Kerantincytes	Cluster0008
Kerantincytes	Cluster0008
Kerantincytes	Cluster0008
Kerantincytes	Cluster0008
Kerantincytes	Cluster0008
Kerantincytes	Cluster0008
Kerantincytes	Cluster0008
Kerantincytes	Cluster0008
Kerantincytes	Cluster0008
Kerantincytes	Cluster0008
Kerantincytes	Cluster0008
Kerantincytes	Cluster0008
Kerantincytes	Cluster0008
Kerantincytes	Cluster0008
Kerantincytes	Cluster0008
Kerantincytes	Cluster0008
Kerantincytes	Cluster0008
Kerantincytes	Cluster0008
Kerantincytes	Cluster0008
Kerantincytes	Cluster0008
Kerantincytes	Cluster0008
Kerantincytes	Cluster0008
Kerantincytes	Cluster0008
Kerantincytes	Cluster0008
Kerantincytes	Cluster0008
Kerantincytes	Cluster0008
Kerantincytes	Cluster0008
Kerantincytes	Cluster0008
Kerantincytes	Cluster0008
Kerantincytes	Cluster0008
Kerantincytes	Cluster0008
Kerantincytes	Cluster0008
Kerantincytes	Cluster0008
Kerantincytes	Cluster0008
Kerantincytes	Cluster0008
Kerantincytes	Cluster0008
Kerantincytes	Cluster0008
Kerantincytes	Cluster0008
Kerantincytes	Cluster0008

Kerantincytes	Cluster0008
Kerantincytes	Cluster0008
Kerantincytes	Cluster0008
Epithelium	Cluster0010
Epithelium	Cluster0010
Epithelium	Cluster0010
Epithelium	Cluster0010
Epithelium	Cluster0010
Epithelium	Cluster0010
Epithelium	Cluster0010
Epithelium	Cluster0010
Epithelium	Cluster0010
Epithelium	Cluster0010
Epithelium	Cluster0010
Epithelium	Cluster0010
Epithelium	Cluster0010
Epithelium	Cluster0010
Epithelium	Cluster0010
Epithelium	Cluster0010
Epithelium	Cluster0010
Epithelium	Cluster0010
Epithelium	Cluster0010
Epithelium	Cluster0010
Epithelium	Cluster0010
Epithelium	Cluster0010
Epithelium	Cluster0010
Epithelium	Cluster0010
Epithelium	Cluster0010
Epithelium	Cluster0010
Epithelium	Cluster0010
Epithelium	Cluster0010
Epithelium	Cluster0010
Epithelium	Cluster0010
Epithelium	Cluster0010
Epithelium	Cluster0010
Epithelium	Cluster0010
Epithelium	Cluster0010
Epithelium	Cluster0010
Epithelium	Cluster0010
Epithelium	Cluster0010
Epithelium	Cluster0010
Epithelium	Cluster0010
Epithelium	Cluster0010
Epithelium	Cluster0010
Epithelium	Cluster0010
Epithelium	Cluster0010
Epithelium	Cluster0010
Epithelium	Cluster0010
Epithelium	Cluster0010
Epithelium	Cluster0010

Epithelium	Cluster0010
Epithelium	Cluster0010
Epithelium	Cluster0010
Epithelium	Cluster0010
Epithelium	Cluster0010
Epithelium	Cluster0010
Epithelium	Cluster0010
Epithelium	Cluster0010
Epithelium	Cluster0010
Epithelium	Cluster0010
Epithelium	Cluster0010
Epithelium	Cluster0010
Epithelium	Cluster0010
Epithelium	Cluster0010
Epithelium	Cluster0010
Epithelium	Cluster0010
Epithelium	Cluster0010
Epithelium	Cluster0010
Epithelium	Cluster0010
Epithelium	Cluster0010
Epithelium	Cluster0010
Epithelium	Cluster0010
Epithelium	Cluster0010
Epithelium	Cluster0010
Epithelium	Cluster0010
Epithelium	Cluster0010
Epithelium	Cluster0010
Epithelium	Cluster0010
Epithelium	Cluster0010
Epithelium	Cluster0010
Epithelium	Cluster0010
Epithelium	Cluster0010
Epithelium	Cluster0010
Epithelium	Cluster0010
MHC_class1	Cluster0035
MHC_class1	Cluster0035
MHC_class1	Cluster0035
MHC_class1	Cluster0035
MHC_class1	Cluster0035
MHC_class1	Cluster0035
MHC_class1	Cluster0035
MHC_class1	Cluster0035
MHC_class1	Cluster0035
MHC_class1	Cluster0035
MHC_class1	Cluster0035
MHC_class1	Cluster0035
MHC_class1	Cluster0035
MHC_class1	Cluster0035
MHC_class1	Cluster0035
MHC_class1	Cluster0035

MHC_class1	Cluster0035
MHC_class1	Cluster0035
Hepatocytes	Cluster0042
Hepatocytes	Cluster0042
Hepatocytes	Cluster0042
Hepatocytes	Cluster0042
Hepatocytes	Cluster0042
Hepatocytes	Cluster0042
Hepatocytes	Cluster0042
Hepatocytes	Cluster0042
Hepatocytes	Cluster0042
Hepatocytes	Cluster0042
Hepatocytes	Cluster0042
Hepatocytes	Cluster0042
Hepatocytes	Cluster0042
Hepatocytes	Cluster0042
Hepatocytes	Cluster0042
Hepatocytes	Cluster0042
Neurones	Cluster0044
Neurones	Cluster0044
Neurones	Cluster0044
Neurones	Cluster0044
Neurones	Cluster0044
Neurones	Cluster0044
Neurones	Cluster0044
Neurones	Cluster0044
Neurones	Cluster0044
Neurones	Cluster0044
Neurones	Cluster0044
Neurones	Cluster0044
Neurones	Cluster0044
Neurones	Cluster0044
Neurones	Cluster0044
Neurones	Cluster0044
Neurones	Cluster0044
MHC_class2	Cluster0047
MHC_class2	Cluster0047
MHC_class2	Cluster0047
MHC_class2	Cluster0047
MHC_class2	Cluster0047
MHC_class2	Cluster0047
MHC_class2	Cluster0047
MHC_class2	Cluster0047
MHC_class2	Cluster0047
MHC_class2	Cluster0047
MHC_class2	Cluster0047
MHC_class2	Cluster0047
MHC_class2	Cluster0047
MHC_class2	Cluster0047
MHC_class2	Cluster0047
Epithelium:keratinocytes	Cluster0048

Epithelium:keratinocytes	Cluster0048
Epithelium:keratinocytes	Cluster0048
Epithelium:keratinocytes	Cluster0048
Epithelium:keratinocytes	Cluster0048
Epithelium:keratinocytes	Cluster0048
Epithelium:keratinocytes	Cluster0048
Epithelium:keratinocytes	Cluster0048
Epithelium:keratinocytes	Cluster0048
Epithelium:keratinocytes	Cluster0048
Epithelium:keratinocytes	Cluster0048
Epithelium:keratinocytes	Cluster0048
Epithelium:keratinocytes	Cluster0048
Epithelium:keratinocytes	Cluster0048
Epithelium:keratinocytes	Cluster0048
Epithelium:keratinocytes	Cluster0050
Epithelium:keratinocytes	Cluster0050
Epithelium:keratinocytes	Cluster0050
Epithelium:keratinocytes	Cluster0050
Epithelium:keratinocytes	Cluster0050
Epithelium:keratinocytes	Cluster0050
Epithelium:keratinocytes	Cluster0050
Epithelium:keratinocytes	Cluster0050
Epithelium:keratinocytes	Cluster0050
Epithelium:keratinocytes	Cluster0050
Epithelium:keratinocytes	Cluster0050
Epithelium:keratinocytes	Cluster0050
Extracellular matrix	Cluster0057
Extracellular matrix	Cluster0057
Extracellular matrix	Cluster0057
Extracellular matrix	Cluster0057
Extracellular matrix	Cluster0057
Extracellular matrix	Cluster0057
Extracellular matrix	Cluster0057
Extracellular matrix	Cluster0057
Extracellular matrix	Cluster0057
Extracellular matrix	Cluster0057
Extracellular matrix	Cluster0057
Adipocytes	Cluster0060
Adipocytes	Cluster0060
Adipocytes	Cluster0060
Adipocytes	Cluster0060
Adipocytes	Cluster0060
Adipocytes	Cluster0060
Adipocytes	Cluster0060
Adipocytes	Cluster0060
Adipocytes	Cluster0060
Adipocytes	Cluster0060

Adipocytes	Cluster0060
Adipocytes	Cluster0060
Endothelial cells	Cluster0116
Endothelial cells	Cluster0116
Endothelial cells	Cluster0116
Endothelial cells	Cluster0116
Endothelial cells	Cluster0116
Endothelial cells	Cluster0116